Reconstruction of tangentially viewing images in a helical system

T. F. Ming, S. Ohdachi, Y. Suzuki
National Institute for Fusion Science
2013.09.06

Outline

- Background and motivations
  - Merits of tangentially viewing imaging system
  - Tangentially viewing VUV imaging system in LHD
- Image reconstructions
  - Relation of line-integrated image and local emission profile
  - Construction of geometry matrix
    - One-dimensional array
    - Tangentially viewing imaging system
  - Synthetic image with a plausible emission profile
- CT reconstruction by numerical tests with LHD configuration
  - Iwama's type of P-T algorithm
  - Numerical test results
- Experimental results
  - Observation of the distorted emission profile caused by ELM event
- Summary

Background

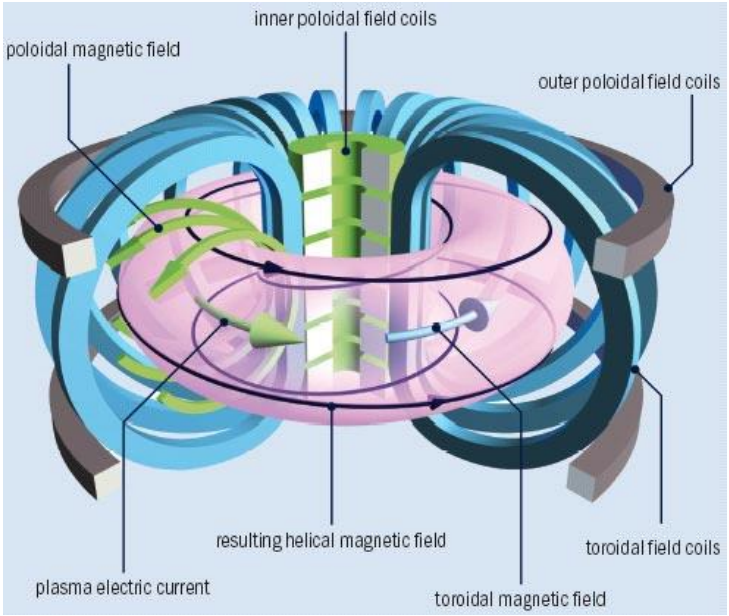

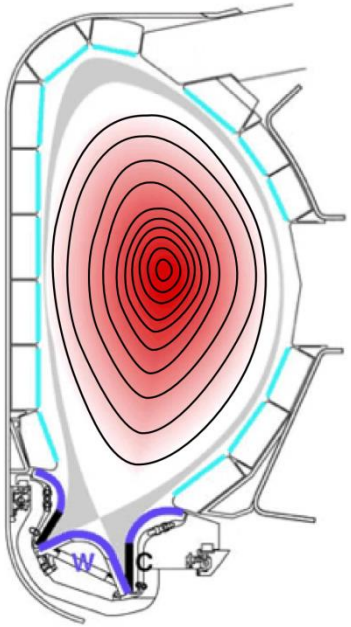

MHD mode structure

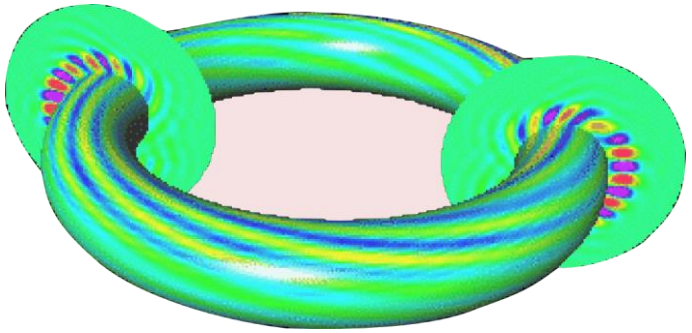

- Plasma is confined by a magnetic configuration produced by the combination of external coils and plasma current.
- Emissivity is approximately constant on each magnetic flux surface.
- Emission profile can be modified by MHD instabilities.

Easier installation of the tangentially viewing imaging system in LHD

J. Mlynar et al, PPCF(2003)

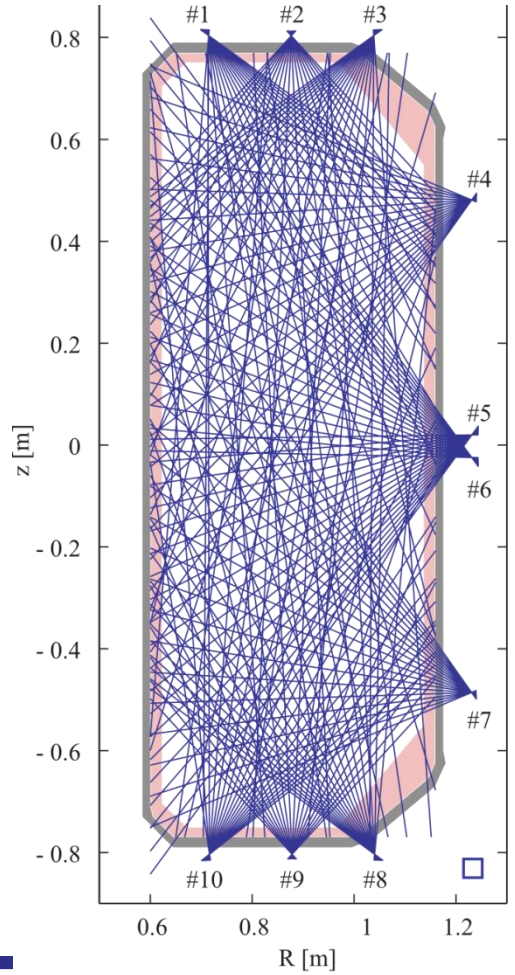

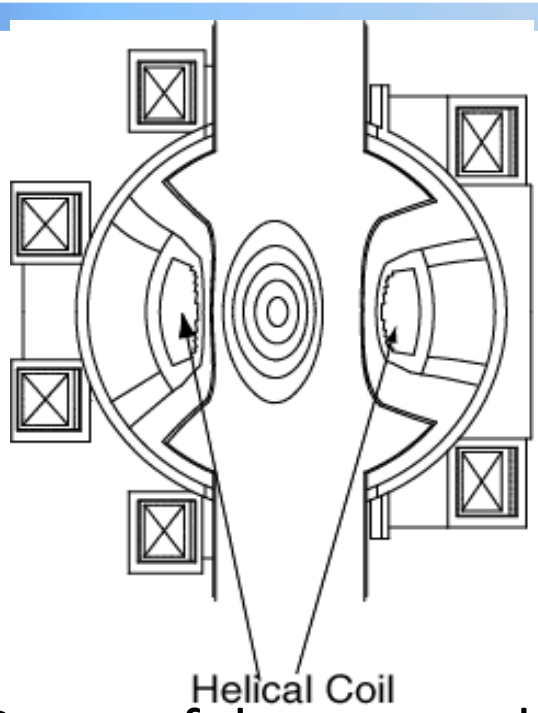

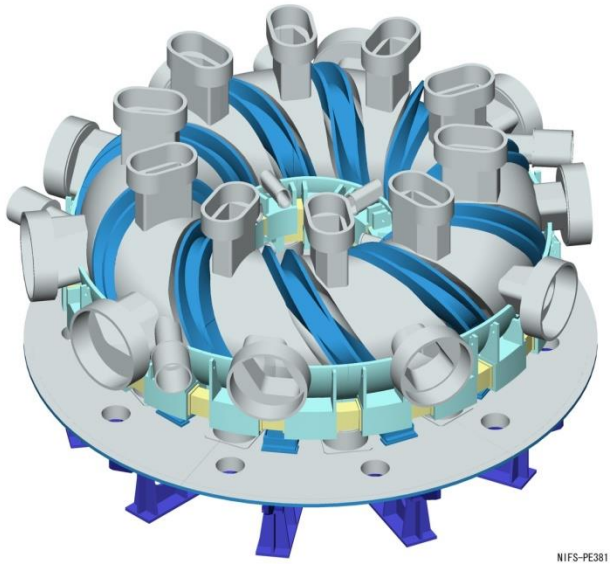

- Successful tomographic reconstruction requires observations from different viewing angles.
- Viewing angles are restrained by the helical coils in LHD.

Schematic diagram of the VUV imaging system

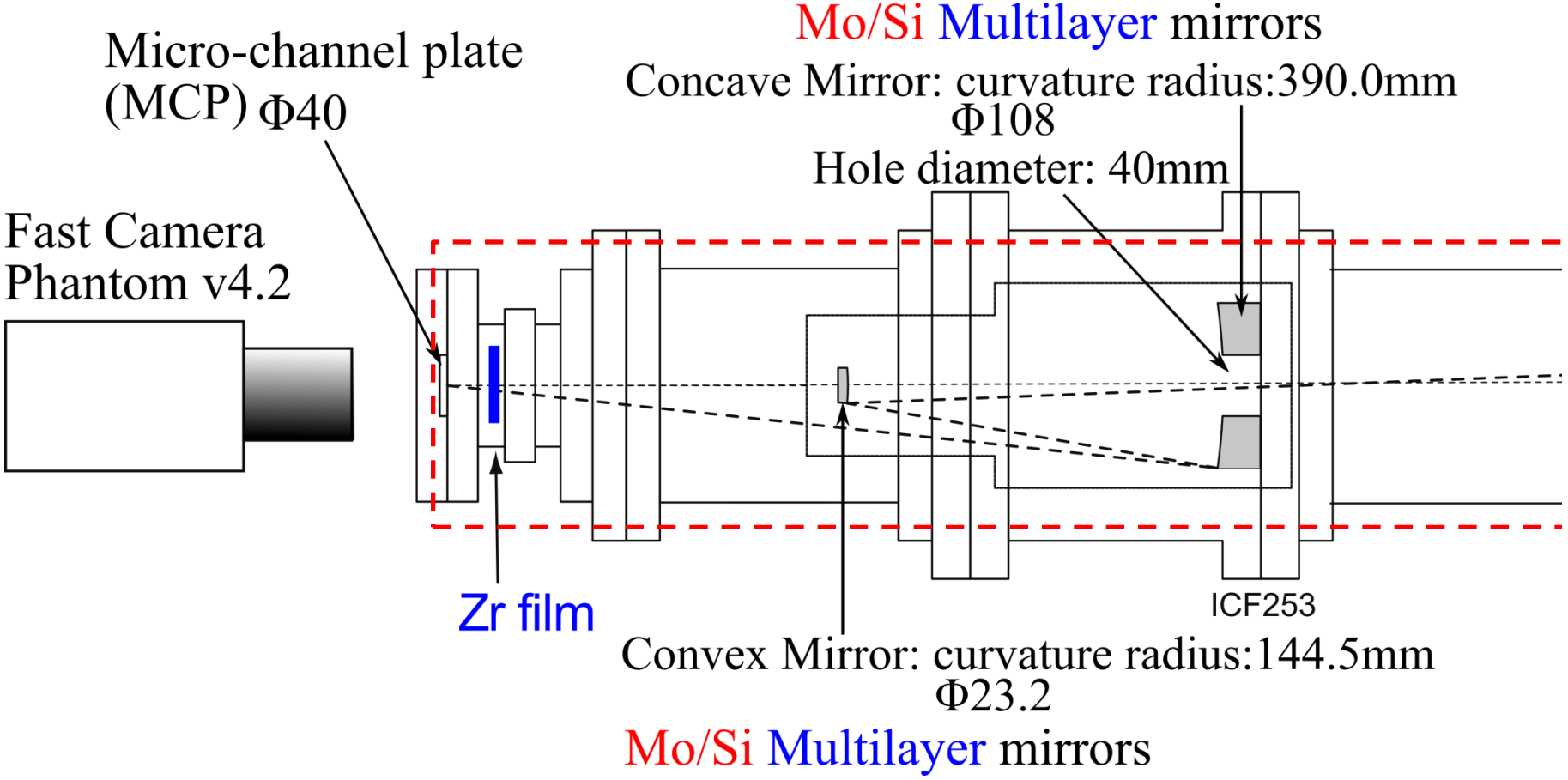

Viewing field of VUV imaging system

- Whole system is installed at the 6-T port of LHD.
- The viewing fields of the VUV imaging system are restrained by the inner diameter of the tube.
- Part of the plasma volume is covered .

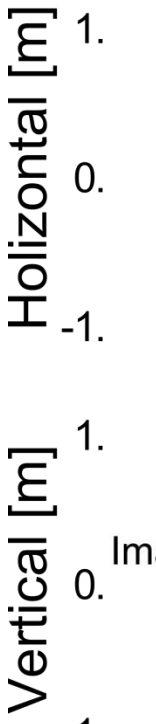

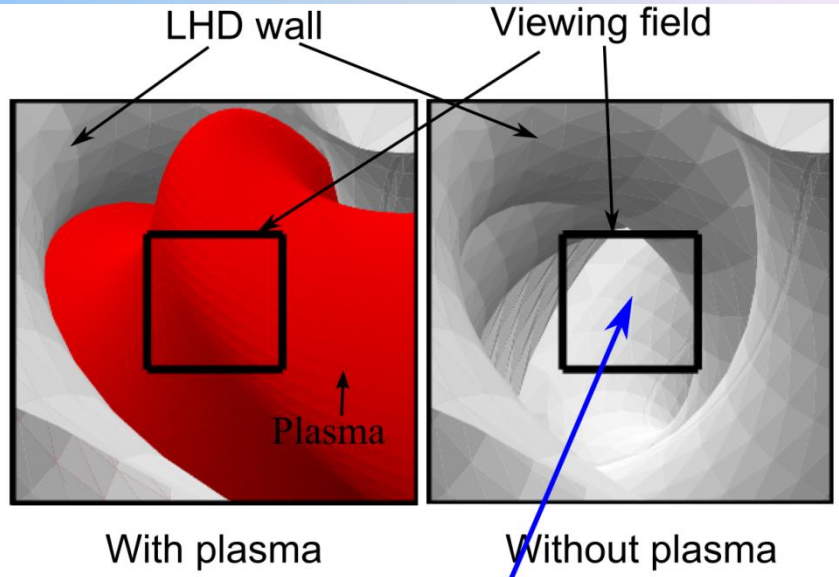

Image taken by a visible camera locating at the focus plane

Outline

- Background and motivations
  - Merits of tangentially viewing imaging system
  - Tangentially viewing VUV imaging system in LHD
- Image reconstructions
  - Relation of line-integrated image and local emission profile
  - Construction of geometry matrix
    - One-dimensional array
    - Tangentially viewing imaging system
  - Synthetic image with a plausible emission profile
- CT reconstruction by numerical tests with LHD configuration
  - Iwama's type of P-T algorithm
  - Numerical test results
- Experimental results
  - Observation of the distorted emission profile caused by ELM event
- Summary

Relation between local emissivity and line-integrated measurements

For a 2D emission profile $E(x,y)$, the *i'th* nonlocal measurement I_i can be described by

$$I_i = \int\int S_i(x,y)\, E(x,y)\, dxdy \qquad (1)$$

Measurement | Weight function | Local emissivity

The discrete algebra form of (1) :

$$\mathbf{I} = \mathbf{S}\mathbf{E} \qquad (2)$$

with $\mathbf{I} = \begin{bmatrix} I_1 \\ \cdots \\ I_M \end{bmatrix}$ $\mathbf{E} = \begin{bmatrix} E_1 \\ \cdots \\ E_N \end{bmatrix}$

S_{ij} describes the contribution to the i'th measurement from the j'th grid.

Construction of geometry matrix for 1D array measurement

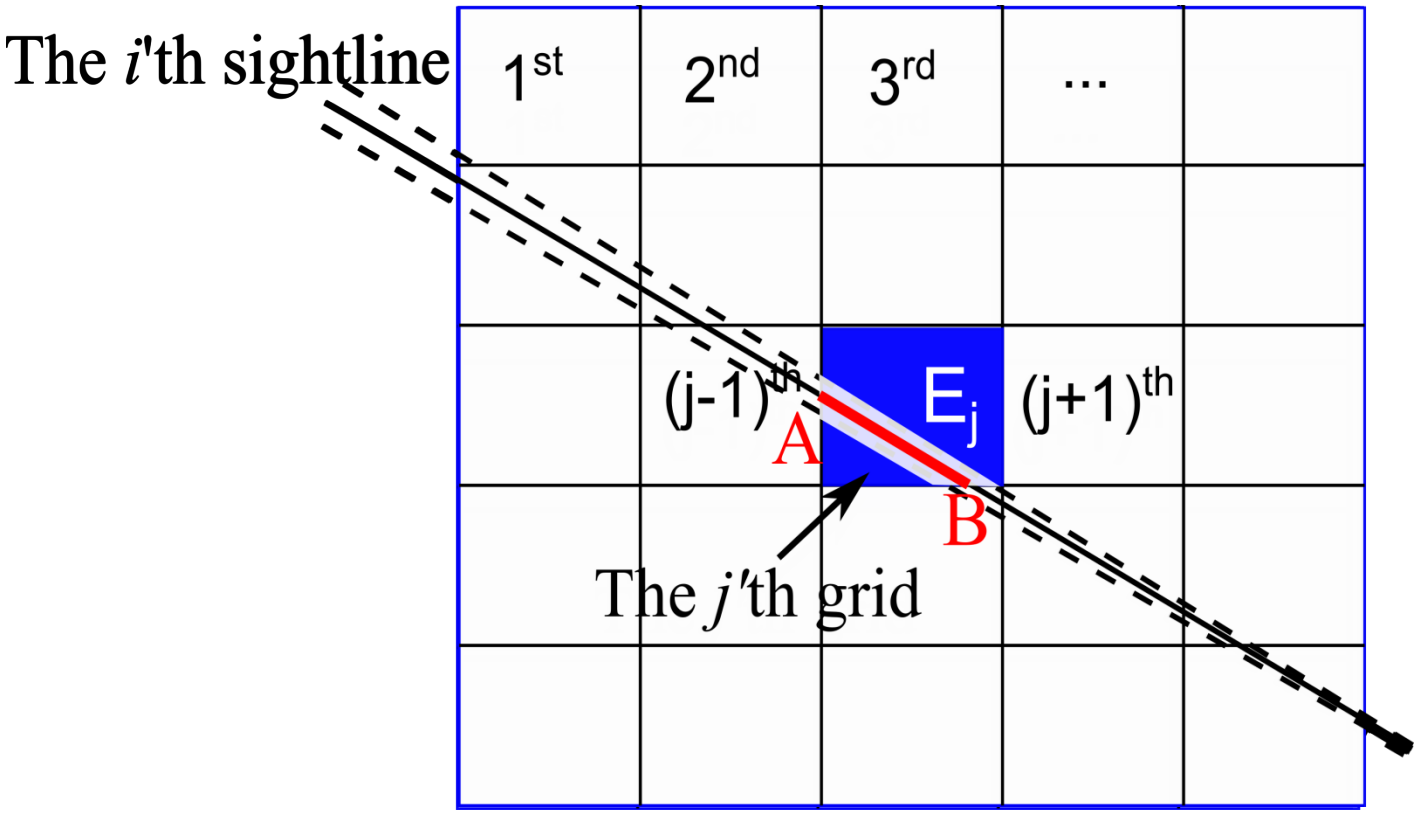

$$S_{ij} \approx |AB|$$

Schematic layout for tangential & array measurements

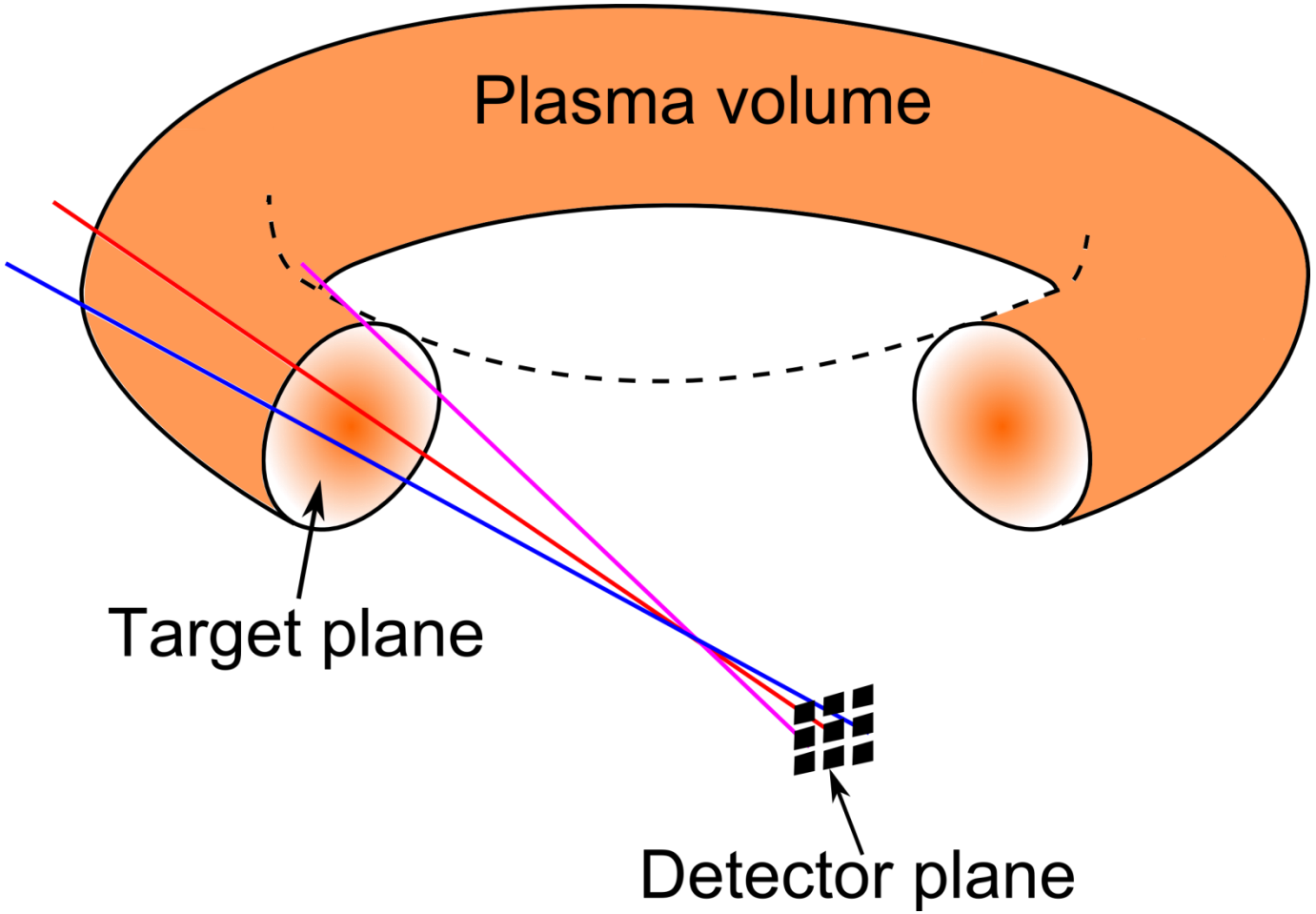

Schematic layout for tangential & array measurements

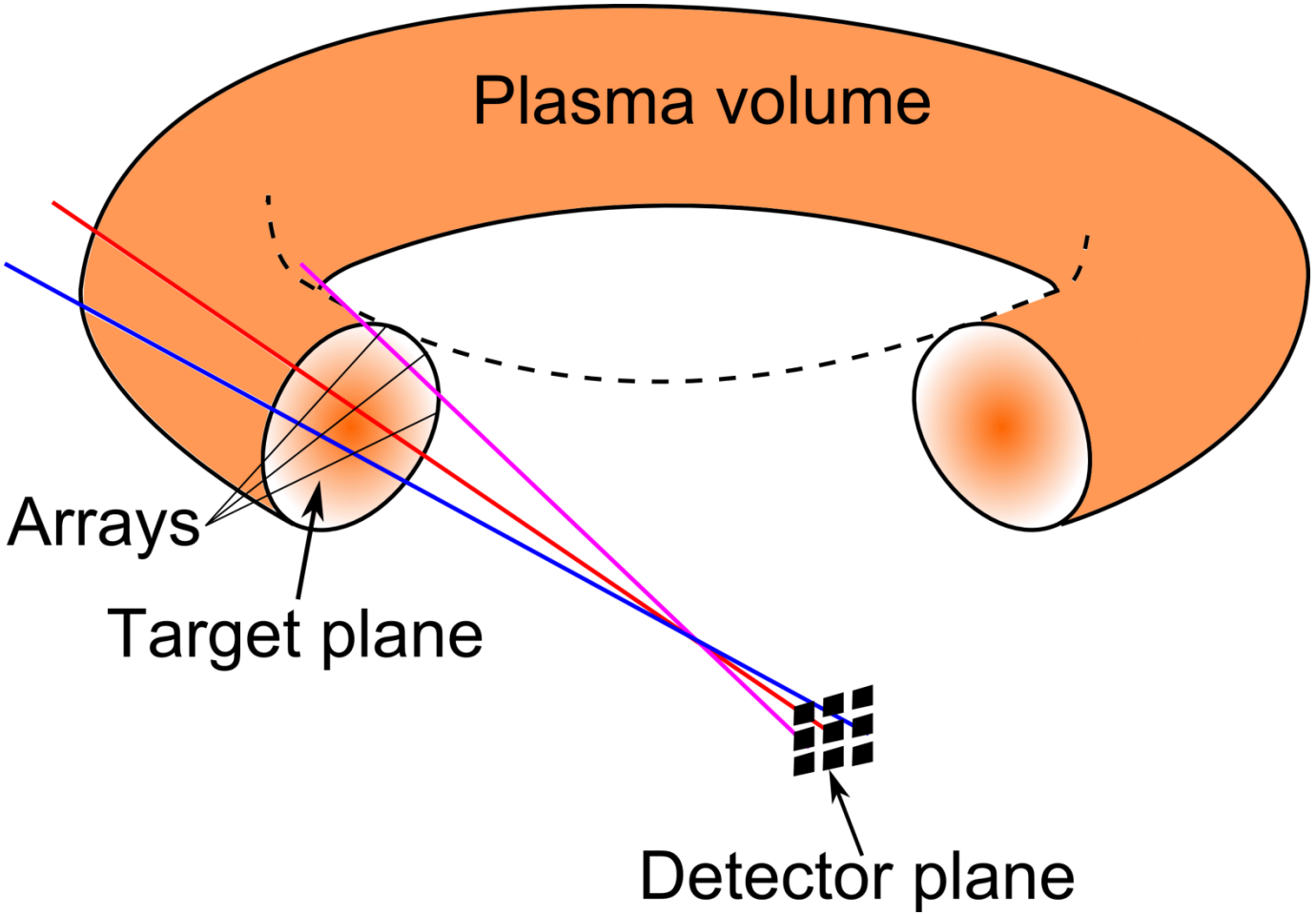

Complex plasma shape in helical device

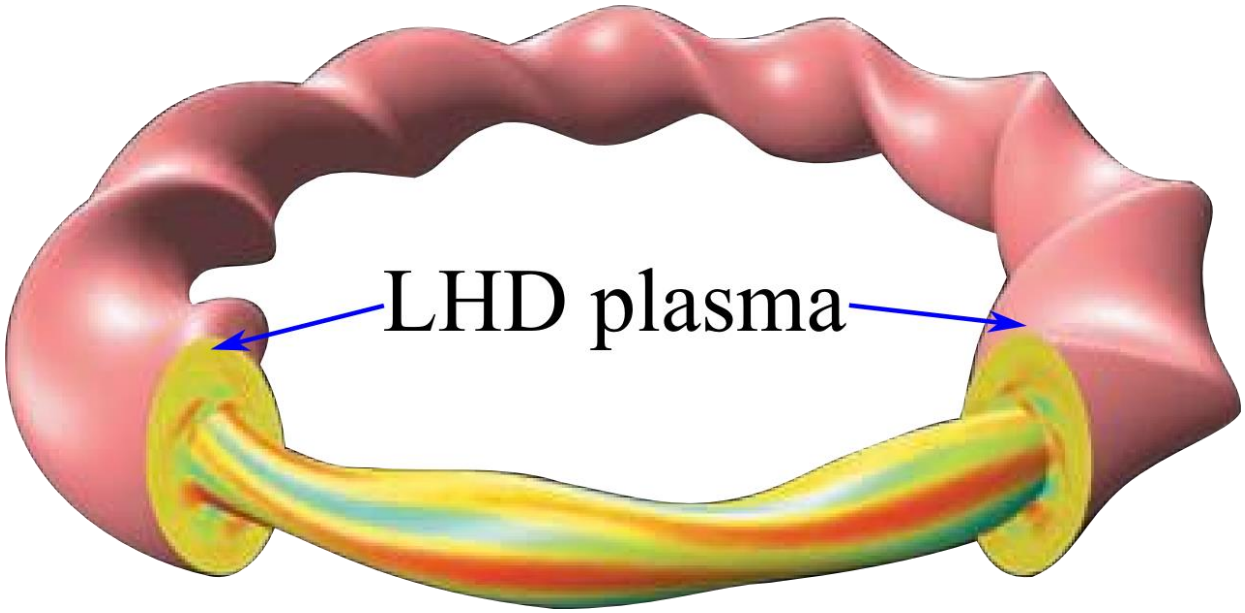

- Plasma volume is helically twisted in LHD.
- No axisymmetry exists in helical configuration.
- How to construct the geometry matrix for a tangentially viewing imaging system with a complex plasma shape?

Construction of geometry matrix for tangentially viewing camera

- The constant emissivity along the magnetic field line is assumed.

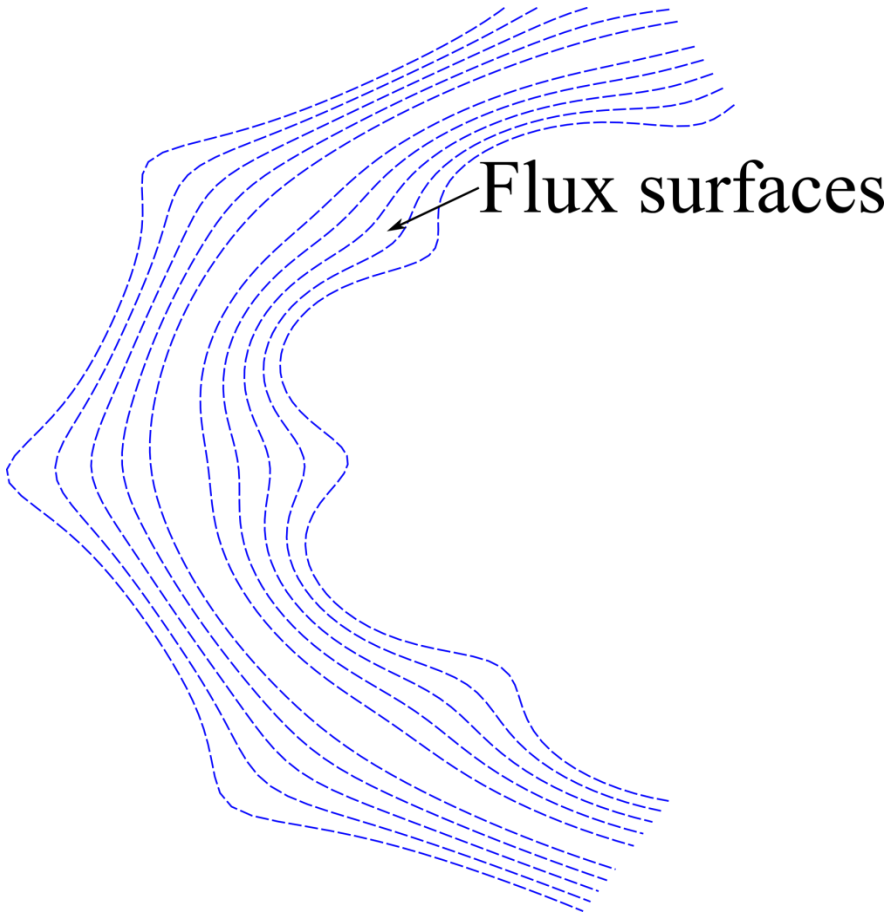

Construction of geometry matrix for tangentially viewing camera

- The constant emissivity along the magnetic field line is assumed.
- The horizontally elongated cross section is selected as the target plane.

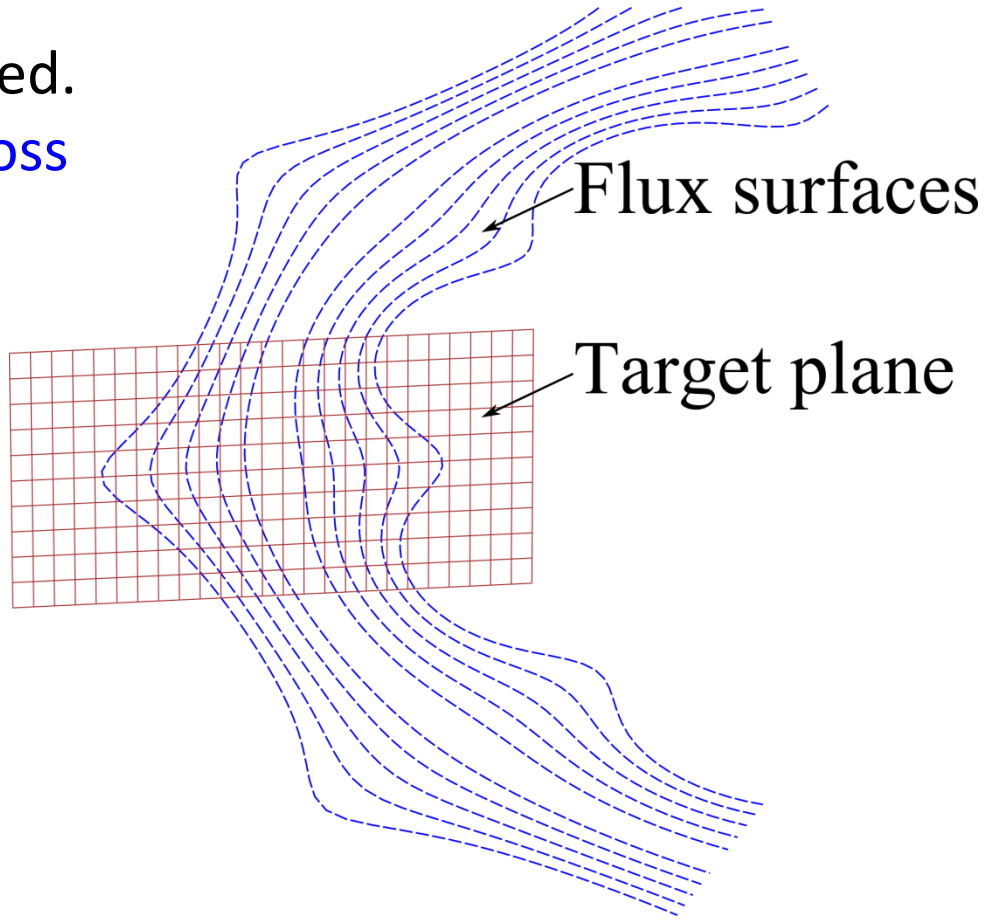

Construction of geometry matrix for tangentially viewing camera

- The constant emissivity along the magnetic field line is assumed.
- The horizontally elongated cross section is selected as the target plane.

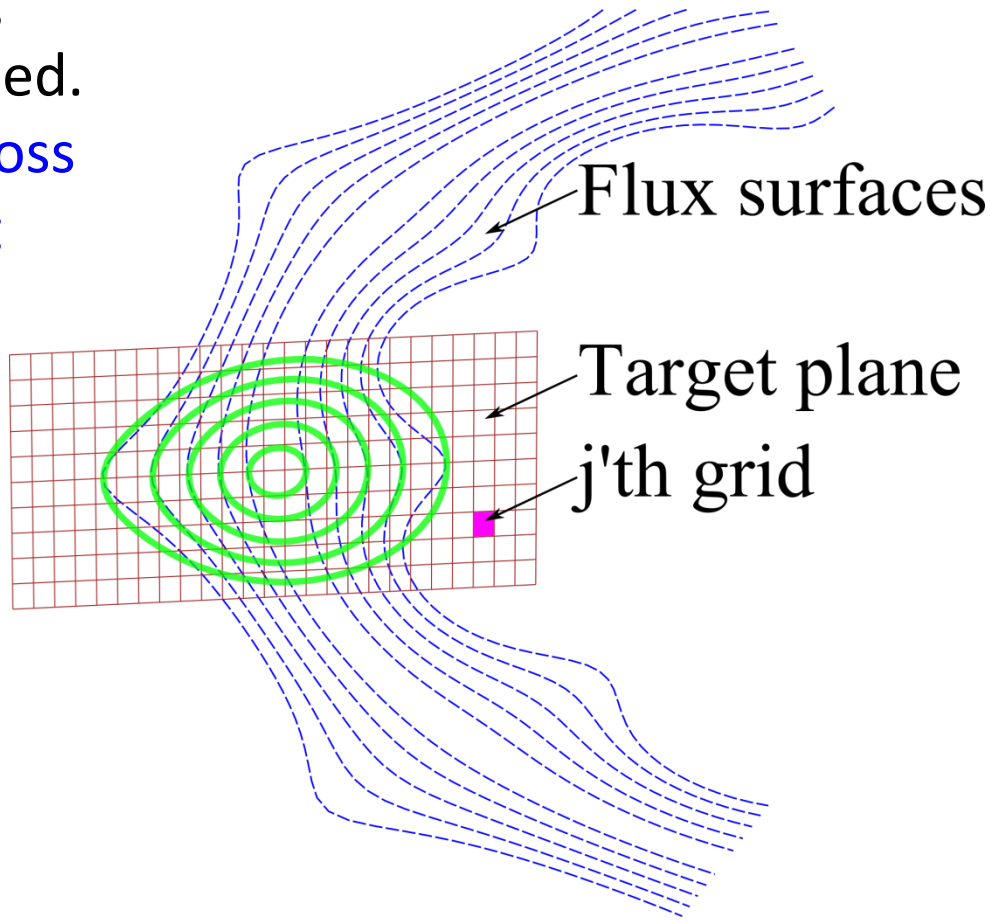

Construction of geometry matrix for tangentially viewing camera

- The constant emissivity along the magnetic field line is assumed.
- The horizontally elongated cross section is selected as the target plane.

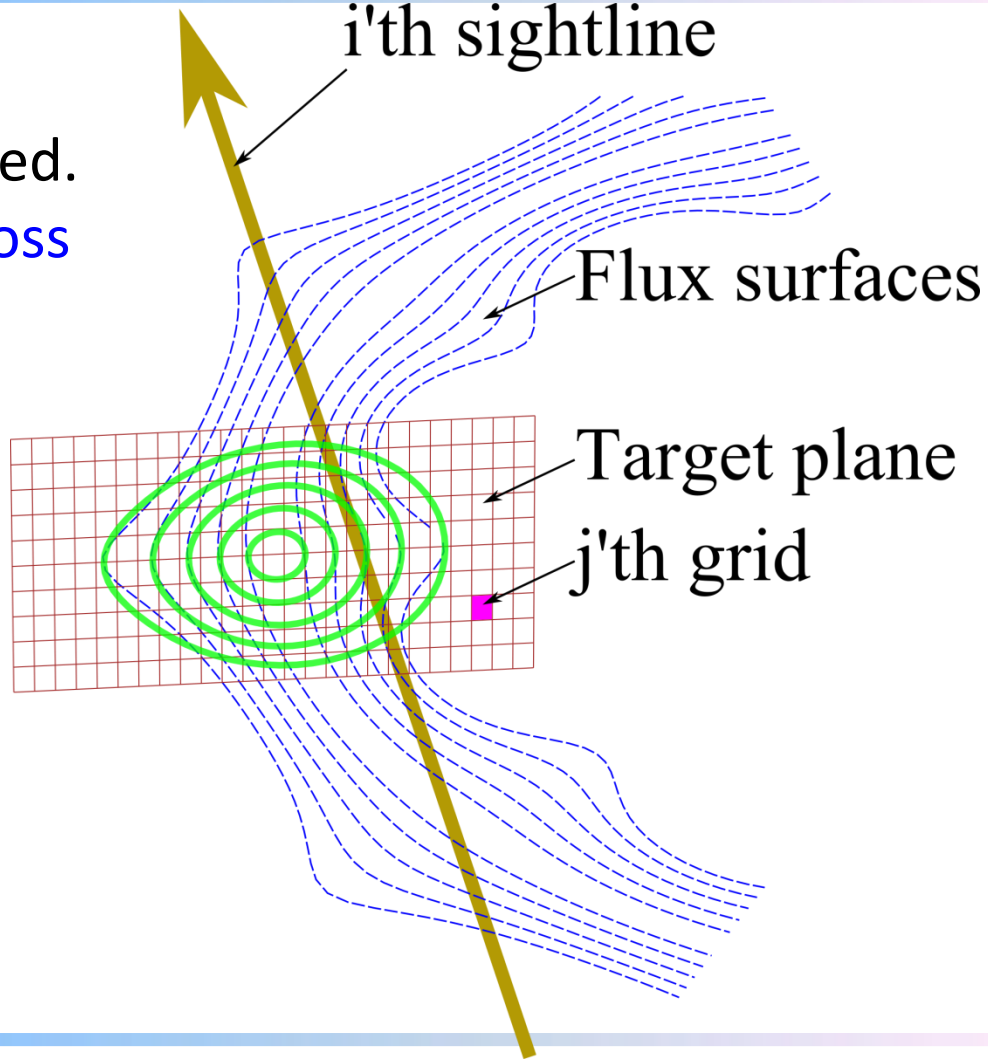

Construction of geometry matrix for tangentially viewing camera

- The constant emissivity along the magnetic field line is assumed.
- The horizontally elongated cross section is selected as the target plane.

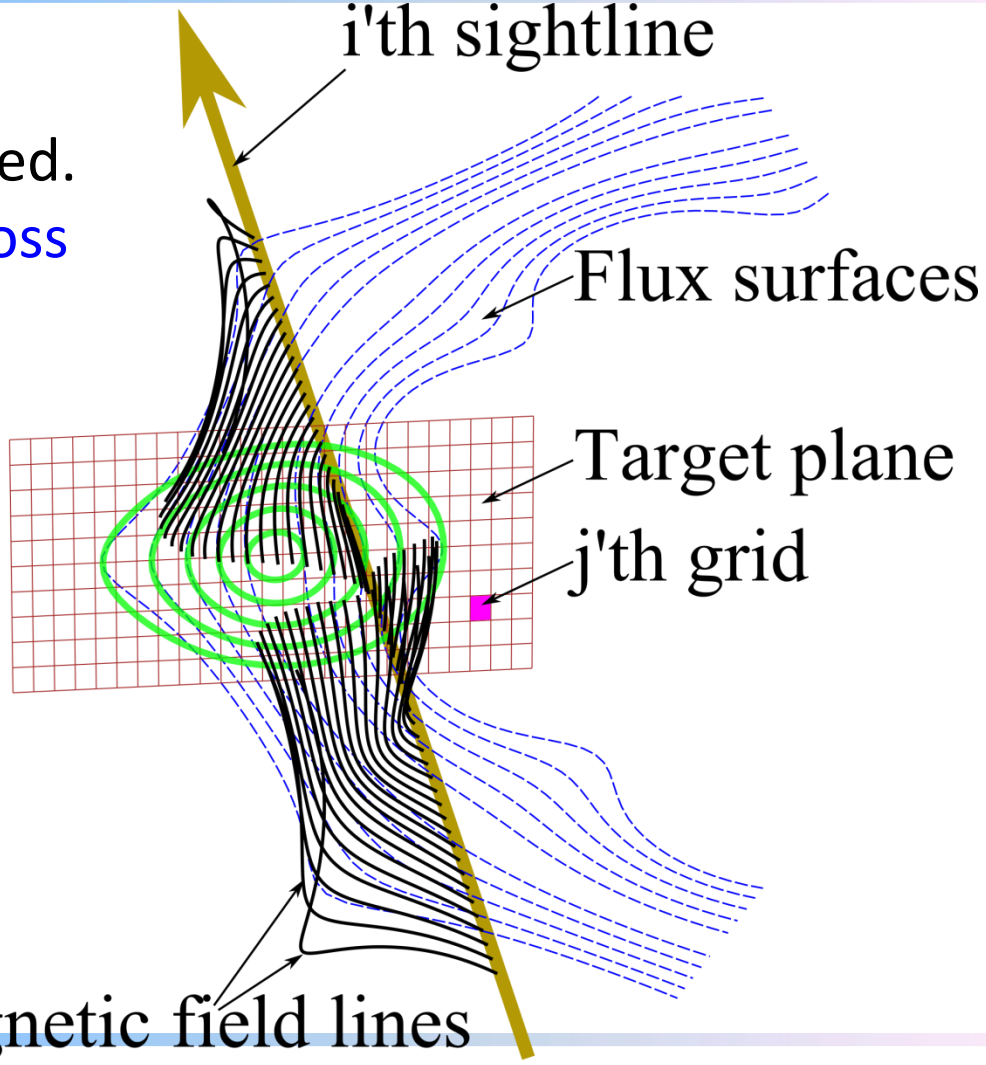

Construction of geometry matrix for tangentially viewing camera

- The constant emissivity along the magnetic field line is assumed.
- The horizontally elongated cross section is selected as the target plane.
- Sightlines are divided into elements with same length, and projected on to the target plane along magnetic field lines.

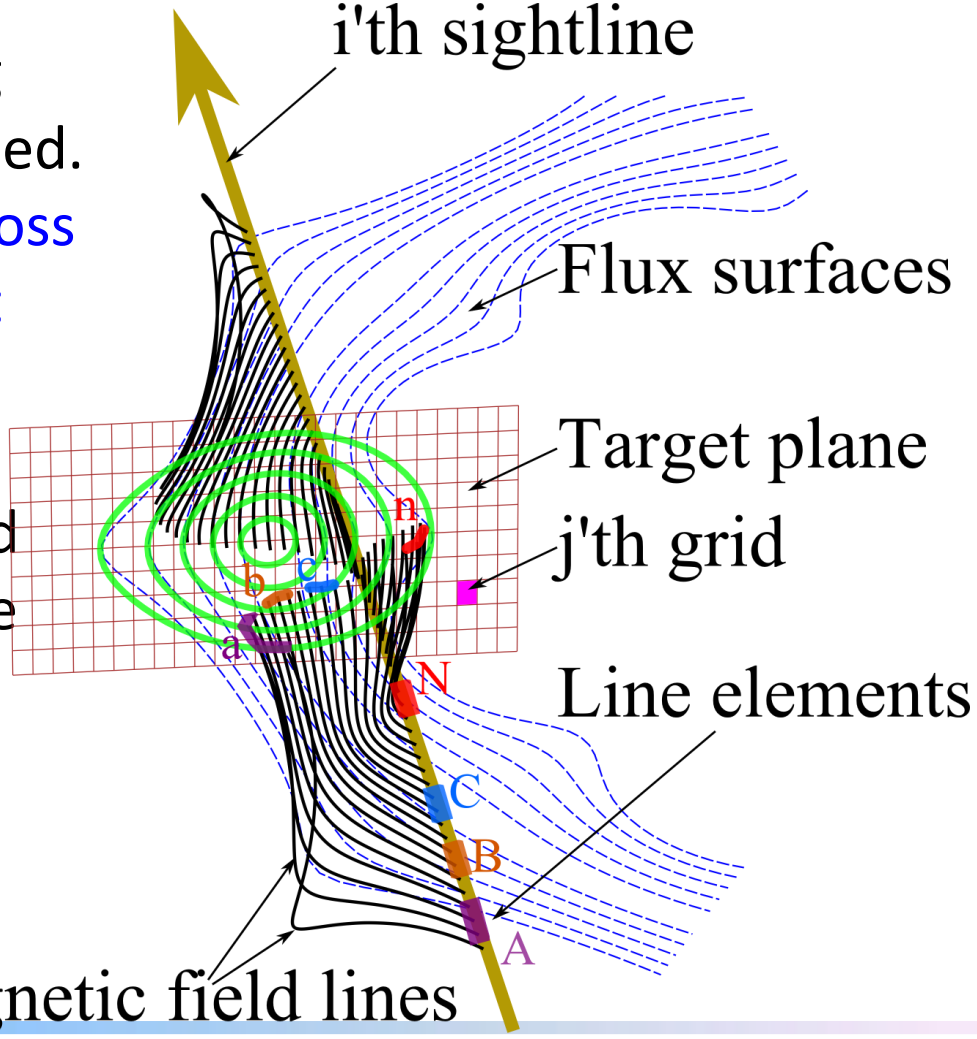

Construction of geometry matrix for tangentially viewing camera

- The constant emissivity along the magnetic field line is assumed.
- The horizontally e
section is selected a
plane.
- Sightlines are divided into elements with same length, and projected on to the target plane along magnetic field lines.
- Equivalent sightline is obtained by relevant projection on the target plane.

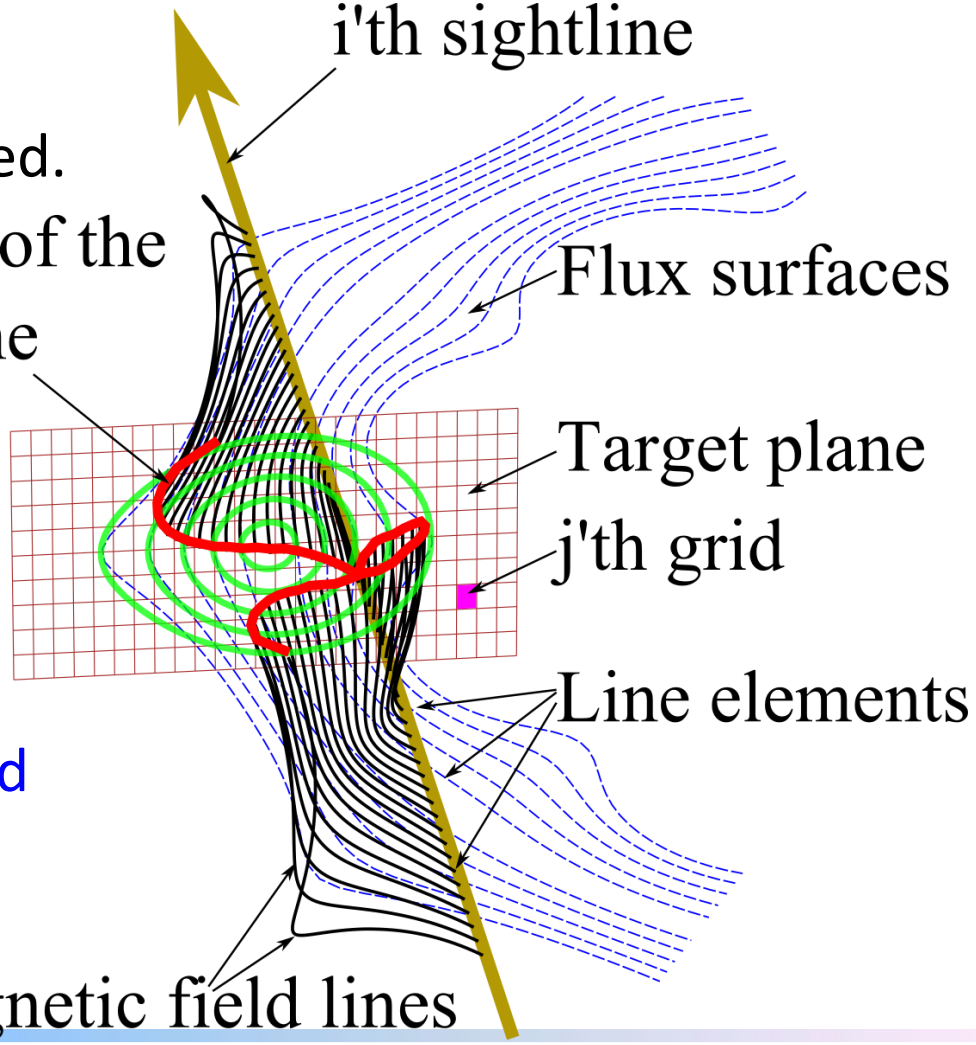

Schematic process of sightline projections

- Line elements are projected forward or backward. It depends on the relative location to the target plane.
- The magnetic filed are obtained using HINT2 equilibrium code.
- Magnetic field lines can be traced with finite beta. And those locating outside the LCFS can also be traced by HINT2.

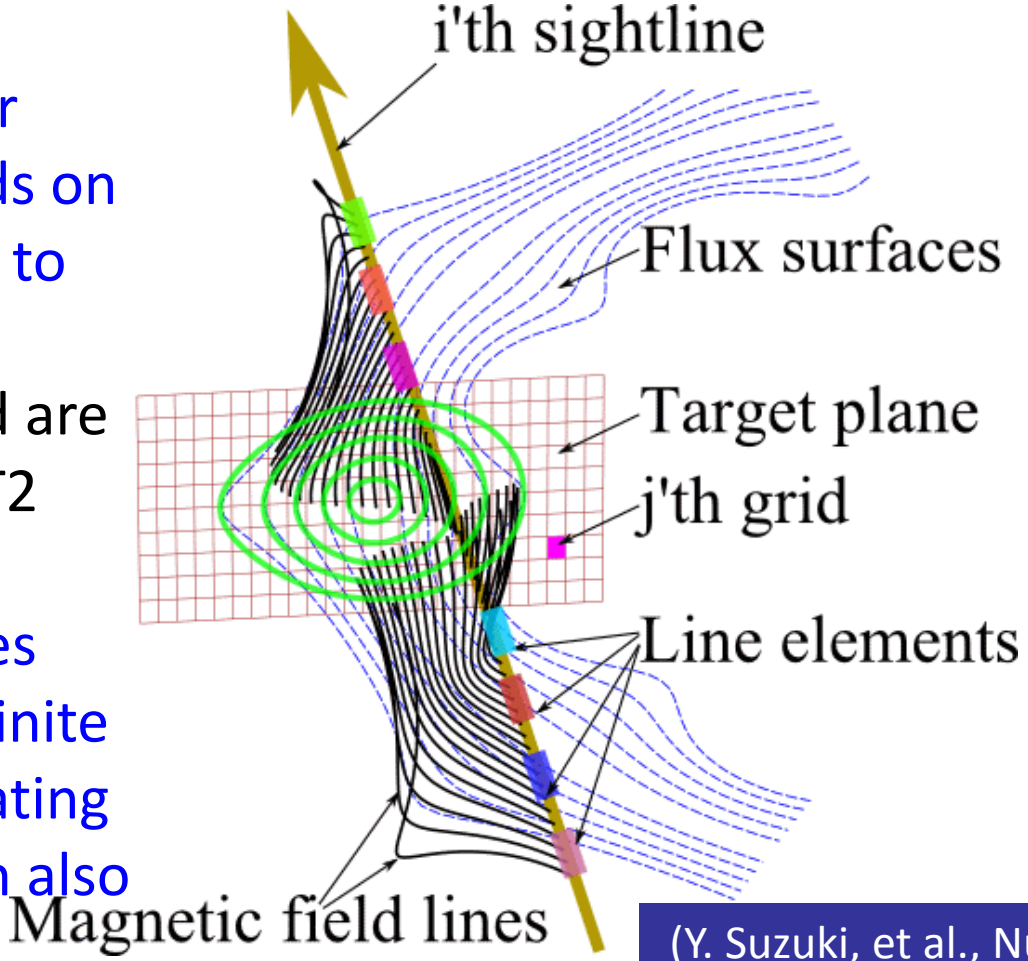

(Y. Suzuki, et al., Nucl. Fusion **46**, L19 (2006),)

Sightline projections on target plane

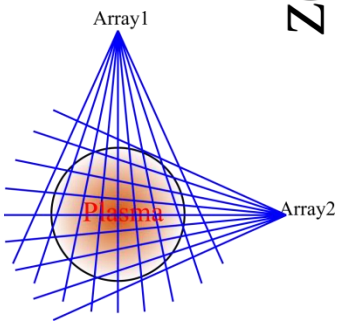

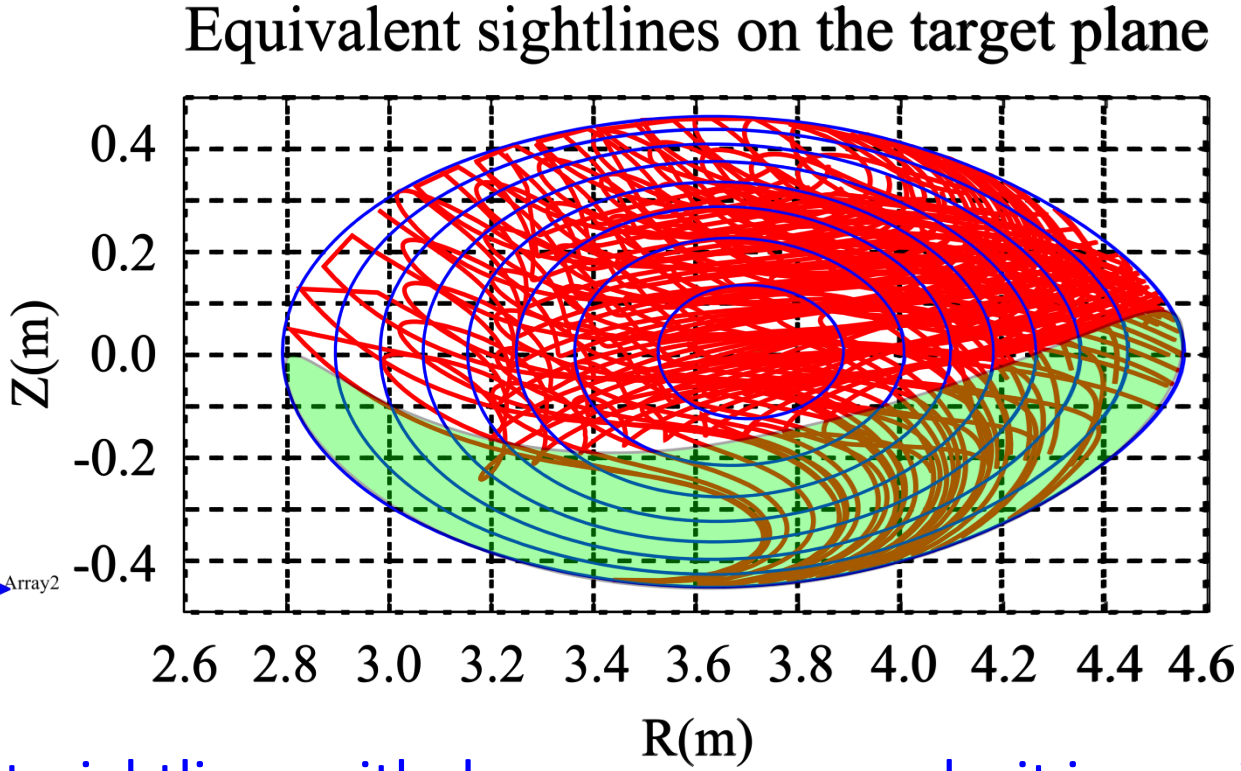

- Equivalent sightlines with dense coverage make it is possible to perform tomographic reconstruction.
- The sparse coverage on the lower part is due to the arrangement of the port.

Intersection between sightlines and the first wall

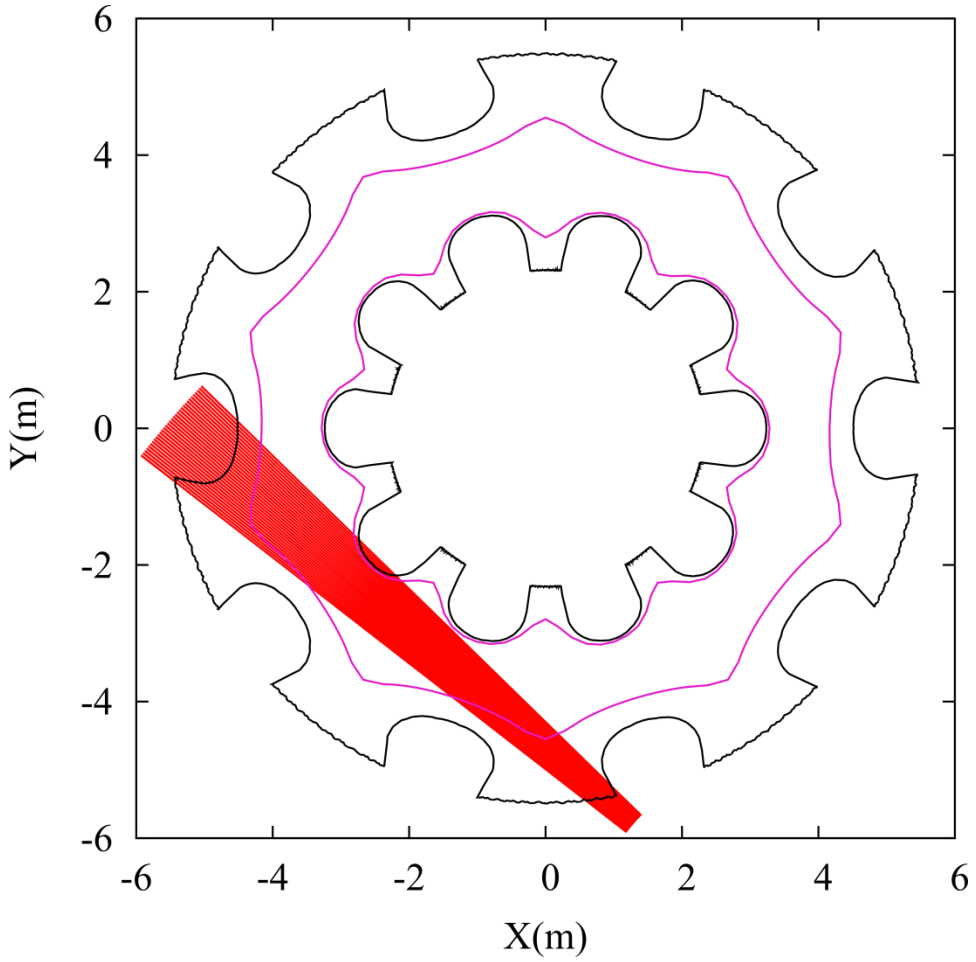

Intersection between sightlines and the first wall

- Intersection between sightlines and the first wall might occur.

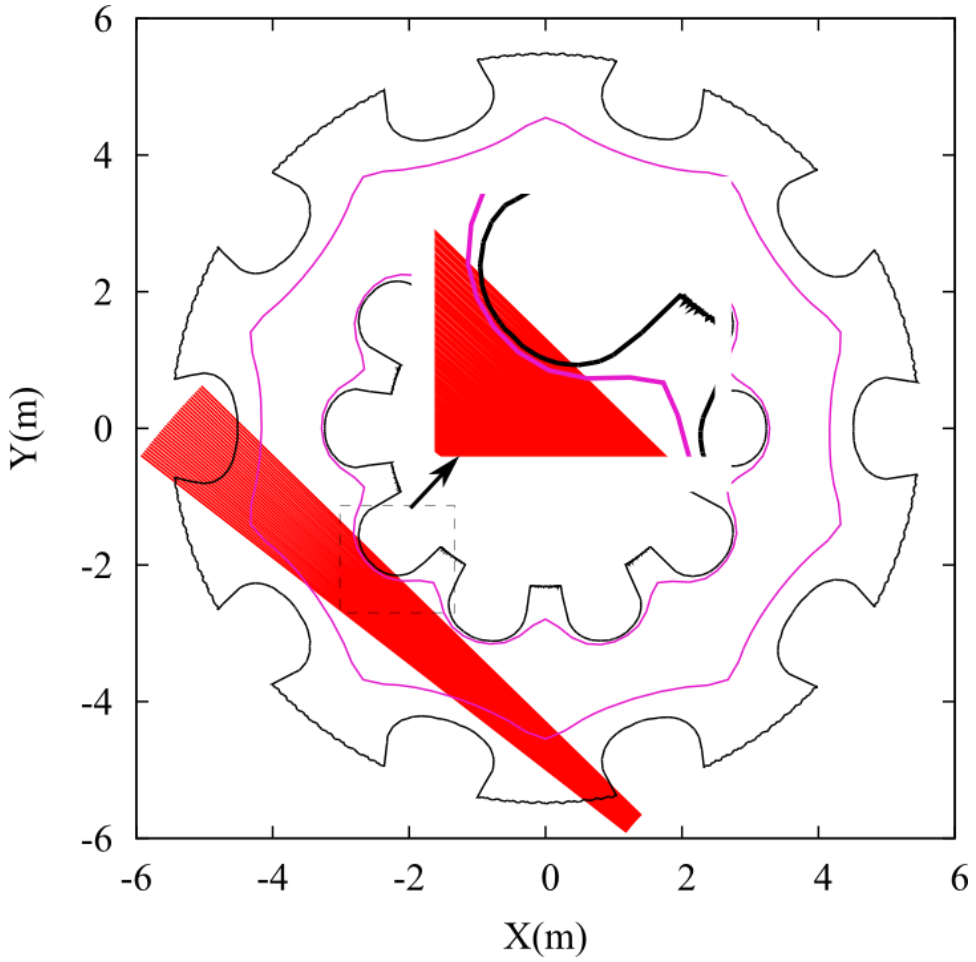

Intersection between sightlines and the first wall

- Intersection between sightlines and the first wall might occur.
- Total length exceeds 9m for each sightline in the calculation.

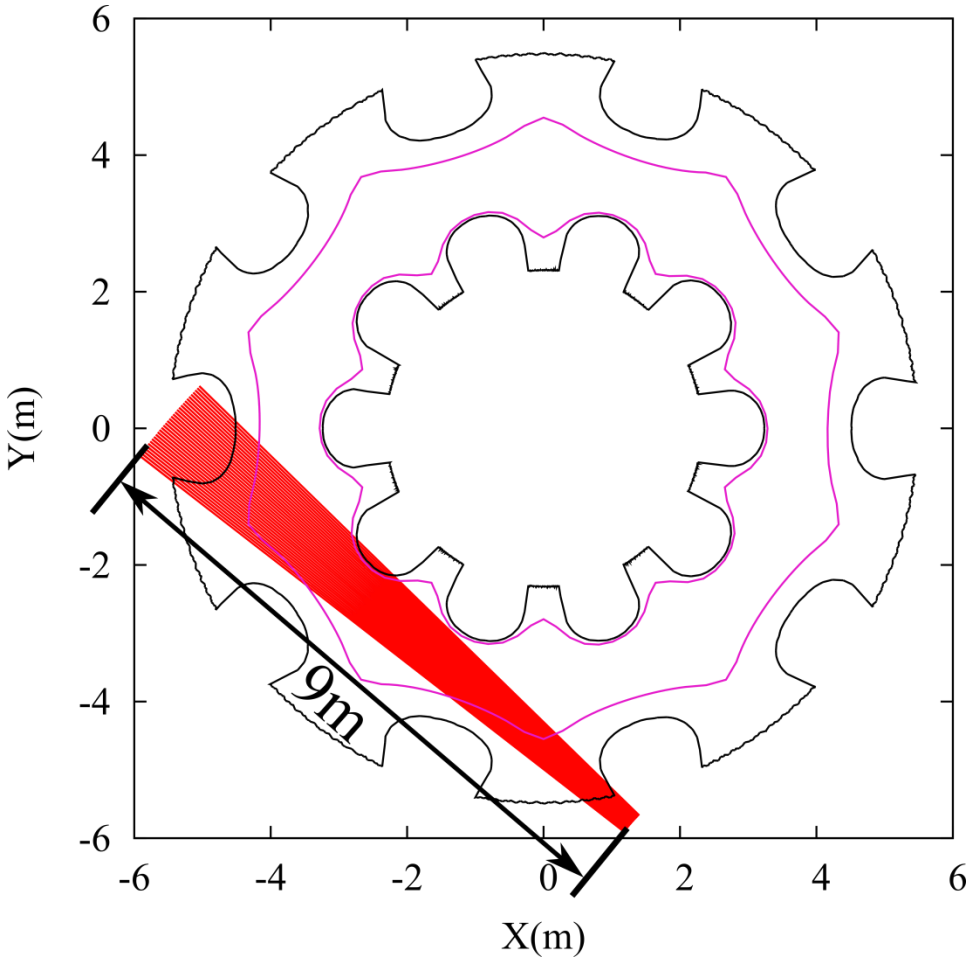

Intersection between sightlines and the first wall

- Intersection between sightlines and the first wall might occur.
- Total length exceeds 9m for each sightline in the calculation.
- The surface of the first wall is simulated by small triangle plate elements. Calculation stops if the intersection occurred.

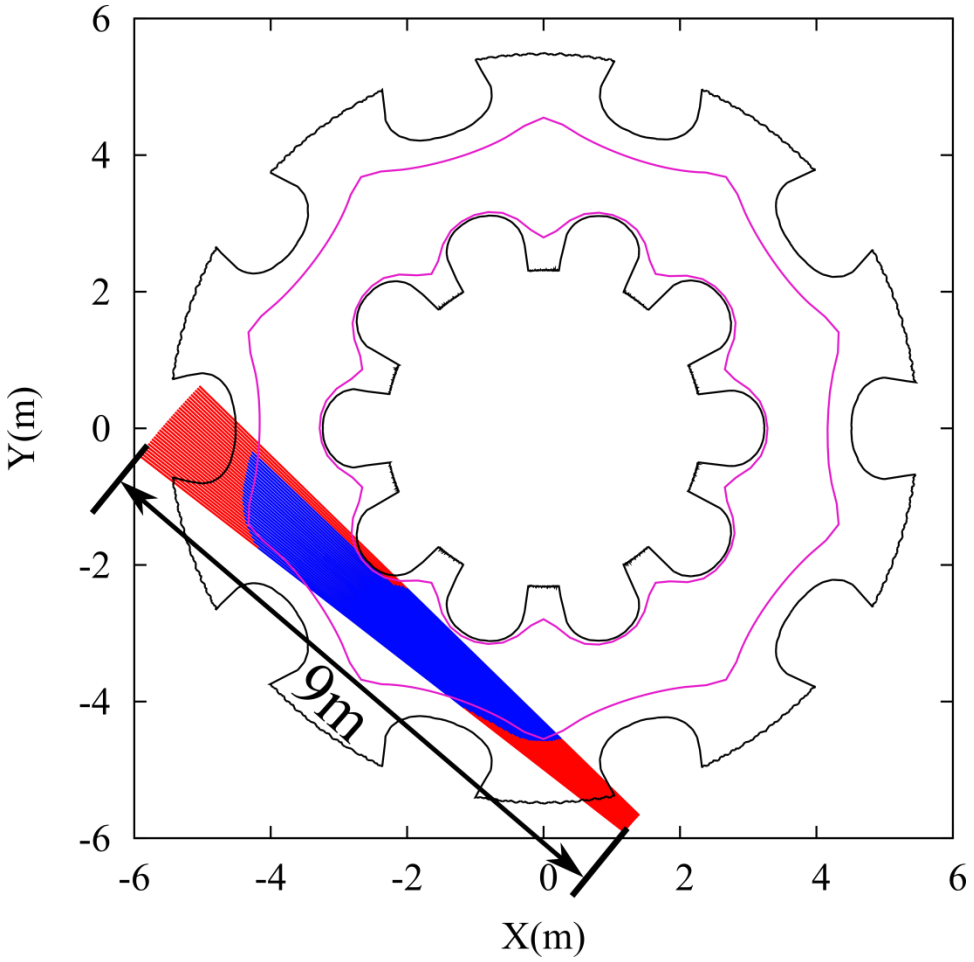

Local emissivity & line-integrated images

Line-integrated image

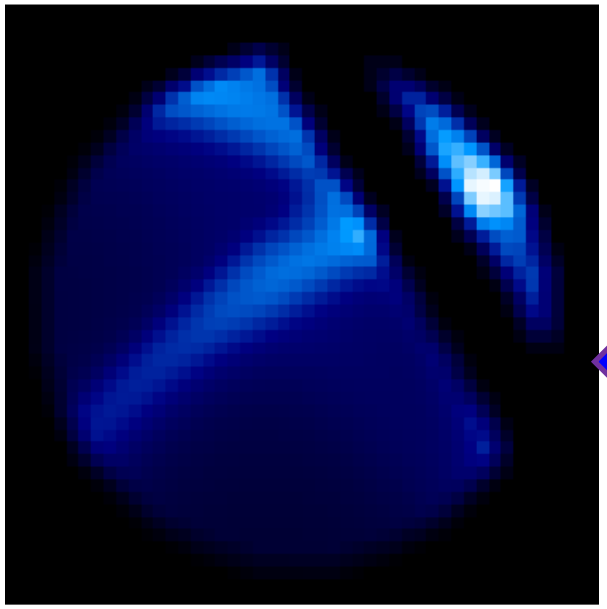

$$\mathbf{I} = \mathbf{SE}$$

Synthetic image

Emissivity

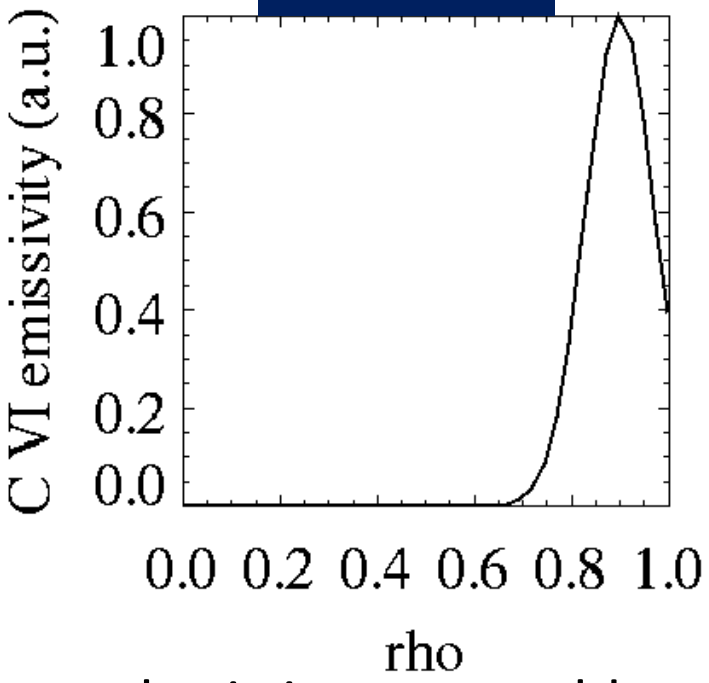

- Assuming local emission profile, relevant synthetic images could be made with the geometry matrix.
- Comparison of the experimental measured images with synthetic ones can be performed.

Synthetic images with different emission profiles

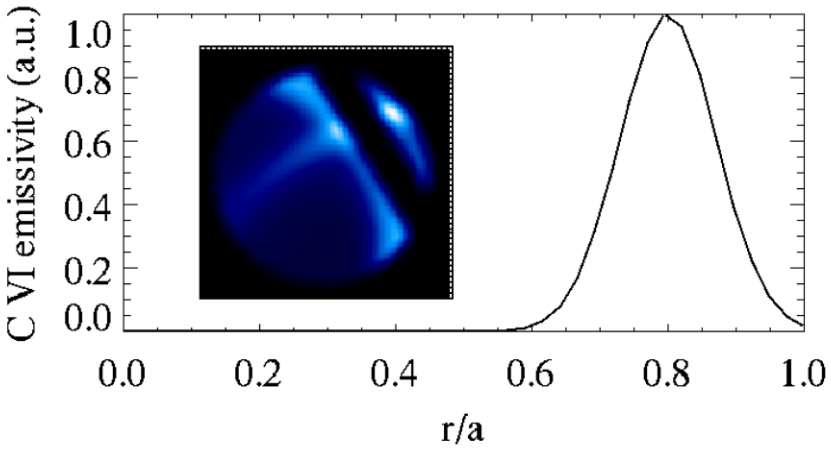

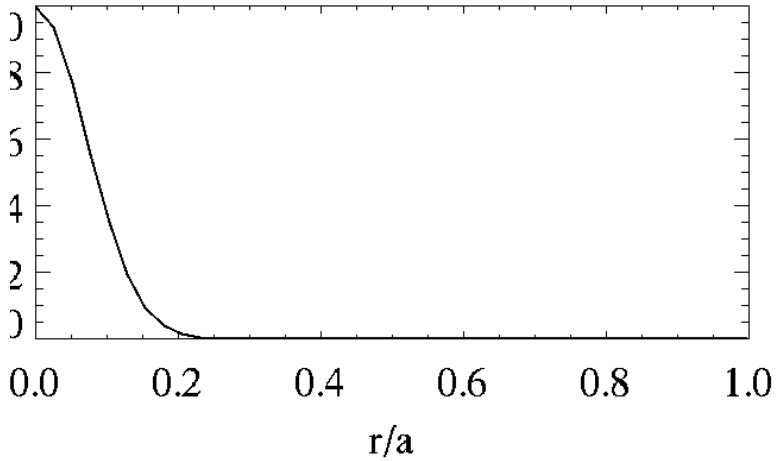

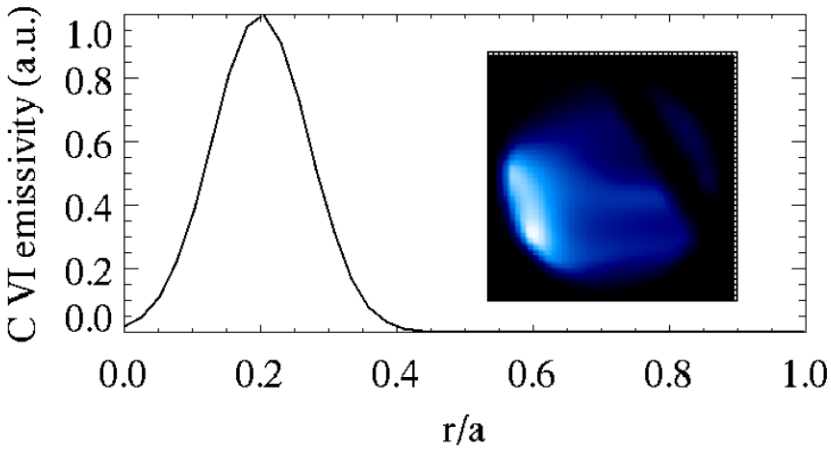

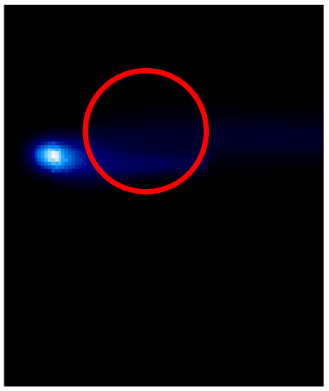

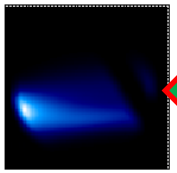

Observed images

- Images are sensitive to the emission profiles, indicating it is good for study on local emission profiles.

Experimental images measured at the beginning of a discharge

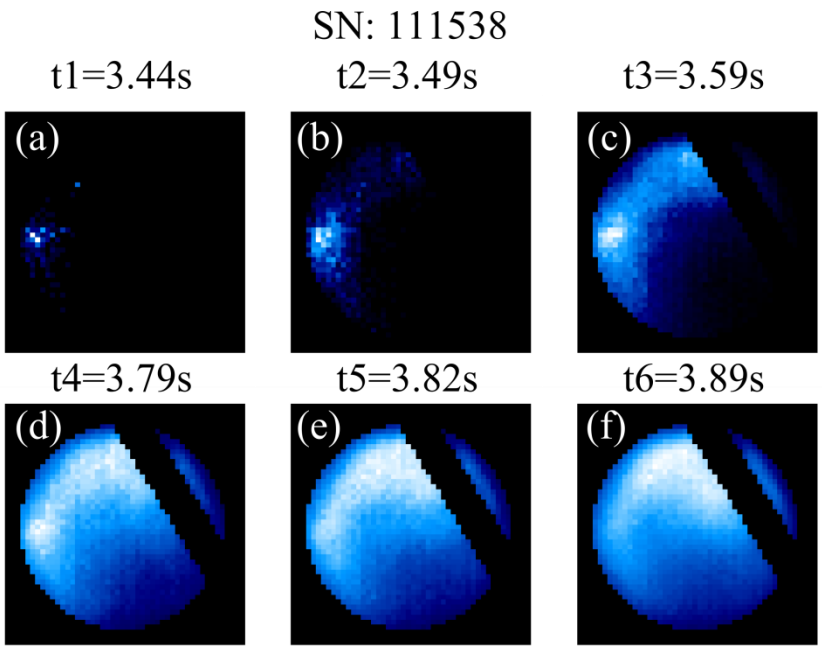

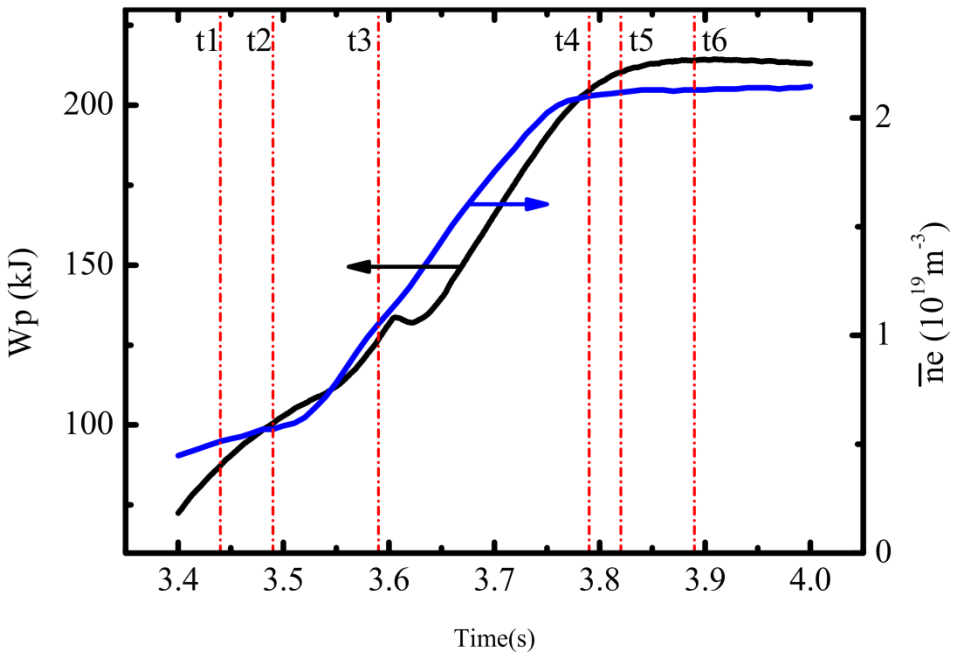

- Plasma expands as the plasma density increases at the startup phase of the discharge.

Outline

- Background and motivations
  - Merits of tangentially viewing imaging system
  - Tangentially viewing VUV imaging system in LHD
- Image reconstructions
  - Relation of line-integrated image and local emission profile
  - Construction of geometry matrix
    - One-dimensional array
    - Tangentially viewing imaging system
  - Synthetic image with a plausible emission profile
- CT reconstruction by numerical tests with LHD configuration
  - Iwama's type of P-T algorithm
  - Numerical test results
- Experimental results
  - Observation of the distorted emission profile caused by ELM event
- Summary

Numerical tests of computed tomographic reconstruction

Line-integrated image

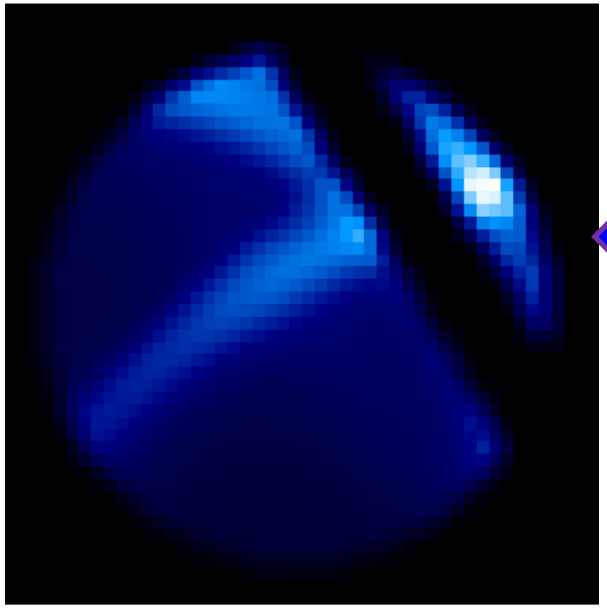

$$\mathbf{I} = \mathbf{SE}$$

Synthetic image

CT reconstruction

?

Phantom

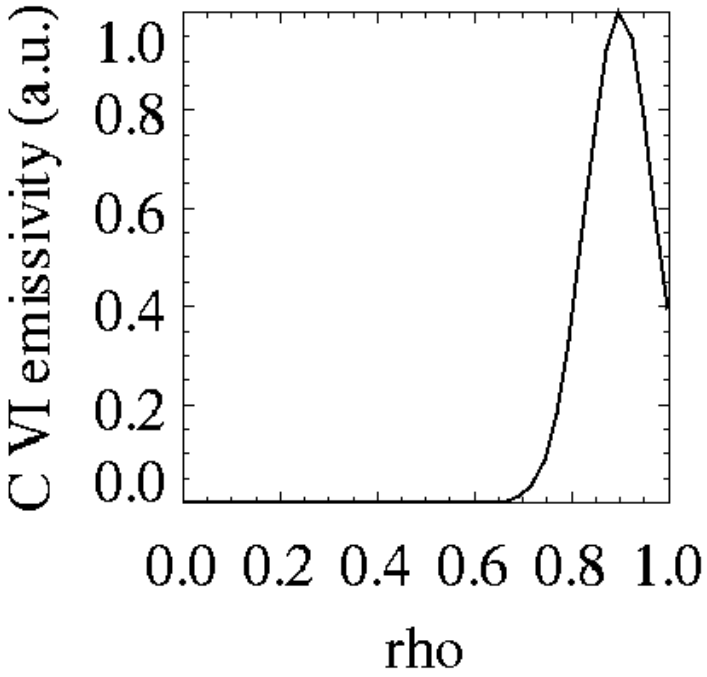

- Assuming a certain phantom, synthetic images could be obtained.
- Can the tomographic reconstruction be successfully performed?

Numerical methods for tomographic image reconstruction

- Inverse Radon Transform (Standard Method of CT)
- Starting from the linear equation: $\mathbf{I} = \mathbf{SE}$
  - Model approach
    - Series Expansion Model (Linear, optimized with AIC, eg: Fourier-Bessel)
  - Model-free approach using penalty functions
    - Phillips-Tikhonov (Linear, optimized with GCV)
    - Maximum Entropy, Hopfield Network

Tomographic reconstruction with penalty functions

- If **S** is not ill-conditioned , then $\mathbf{E} = \left(\mathbf{S}^{\mathbf{T}}\mathbf{S}\right)^{-1}\mathbf{S}^{\mathbf{T}}\mathbf{L}$ if $(\mathrm{S}^{\mathrm{T}}\mathrm{S})^{-1}$exists.
- In tomography (fusion research), Eq.(2) is an ill-conditioned equation.

$$min. \quad J \equiv \| \mathbf{SE} - \mathbf{I} \|^2 + \gamma \; P(E) \quad (3)$$

Least squares error

Penalty function of smoothness

γ is the regularization parameter.

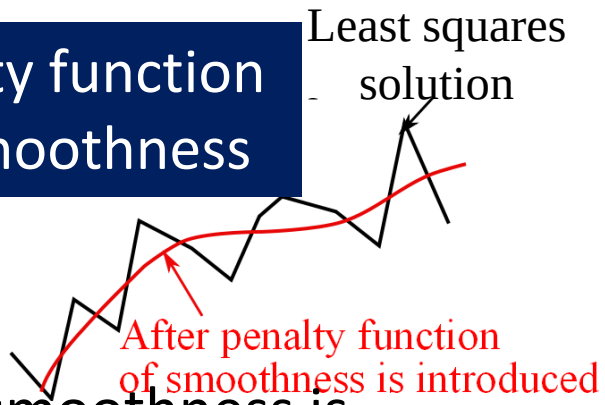

- A minimization of a penalty function P(E) of smoothness is introduced to perform the regularization.
- Several penalty functions are proposed, such as Laplacian, Entropy.

Iwama's type of Phillips-Tikhonov regularization (P-T)

- Linear regularization: $P(E) = \|CE\|^2$

Here, C is the Lapalacian operator.

- Solution:

$$E = \left(S^T S + M\gamma C^T C\right)^{-1} S^T I$$

After the SV decomposition of matrix $C^{-1}S$ in the form:

$$C^{-1}S = U\Sigma V^T$$

$$= \sum_{j=1}^{M} w_j(\gamma) \frac{\left(I, u_j\right)}{\sigma_j} C^{-1} v_j$$

$$w_j(\gamma) = 1/(1 + M\gamma/\sigma_j^2)$$

(*N. Iwama et al, Appl. Phys. Lett.54(6) 502 1989*)

Comparison of Iwama's P-T and Maximum entropy method (MEM)

Method	Penalty function	Computing time	Solution
Iwama's P-T	$\|\|\mathbf{CE}\|\|^2$	~ 0.5 min.	Smooth (Negative value may exist)
MEM	$\sum_{k=1}^{K} E_k ln E_k$	~ 1hour	Smoothness is not good (Always nonnegative)

➢The Iwama's P-T method is selected to investigate the performance of tomographic reconstruction on LHD configuration with phantom tests.

More smooth result can be obtained by Iwama's P-T method

Assumed profile

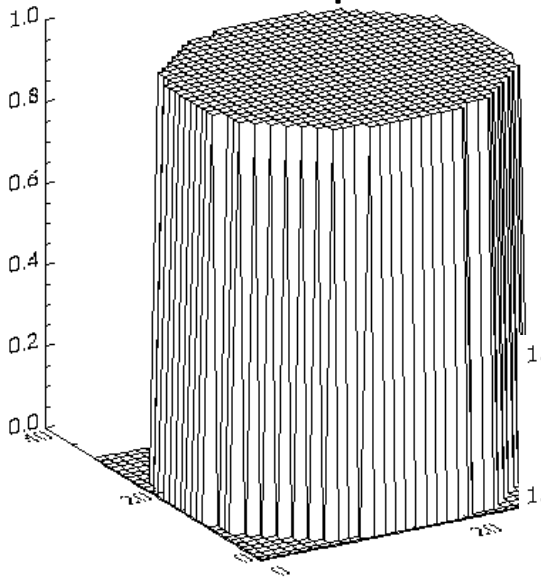

Reconstructed with Iwama's P-T

$d^2 = 0.05$

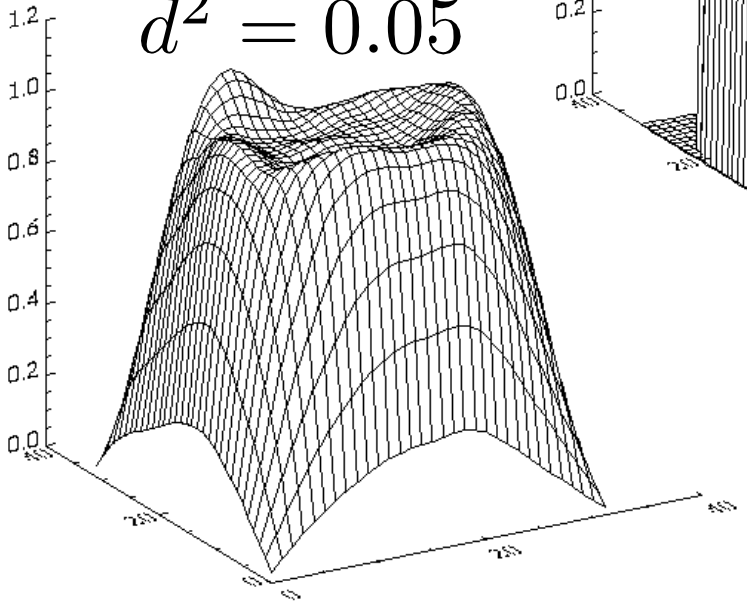

Reconstructed with MEM

$d^2 = 0.08$

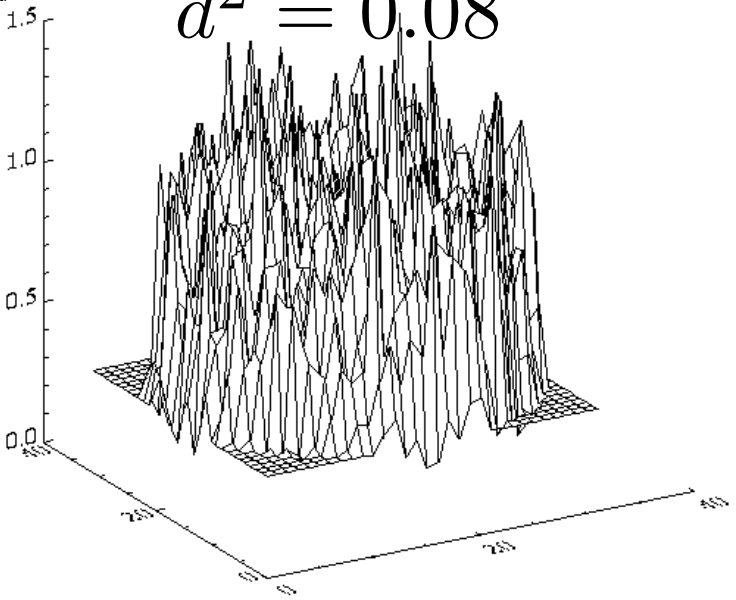

Determination of the optimized regularization parameter γ

➢GCV (Generalized Cross Validation) function is defined as:

$$V(\gamma) = \frac{M \parallel [\mathbf{I_M} - \mathbf{A}(\gamma)]\mathbf{I} \parallel^2}{\{Trace[\mathbf{I_M} - \mathbf{A}(\gamma)]\}}$$

where, $A(\gamma) = \mathbf{S}(\mathbf{S^T S} + M\gamma\mathbf{I_M})^{-1}\mathbf{S^T}$

I_M is the $M \times M$ identity.

➢ From the information theory, minimum GCV is believed to give an optimum solution.

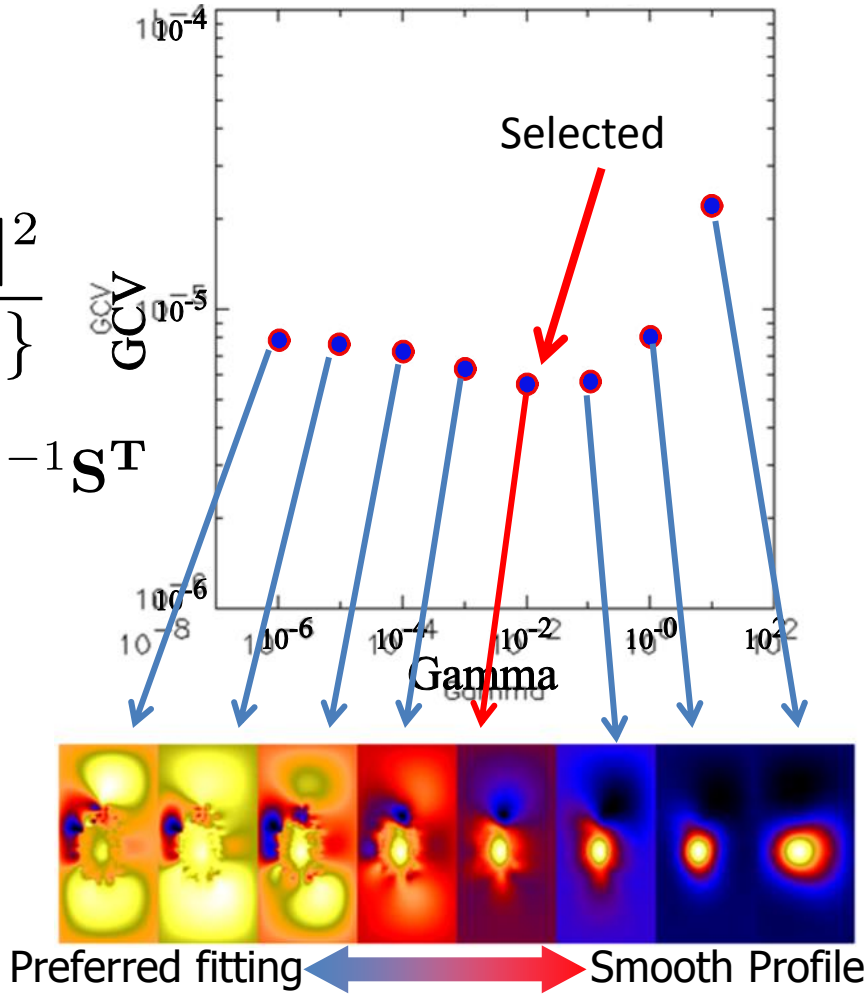

Assumed mode structure

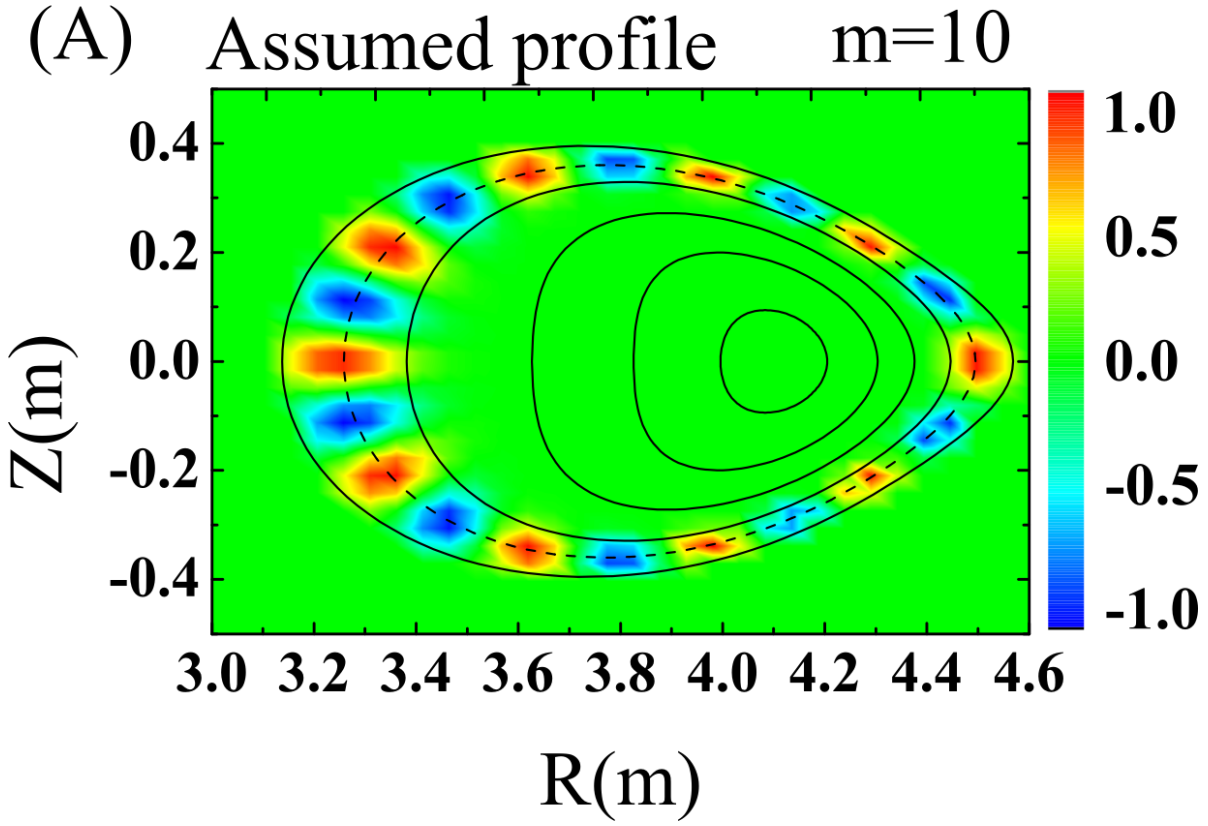

Synthetic images w/wo artificial noise

Without noise

6% noise added

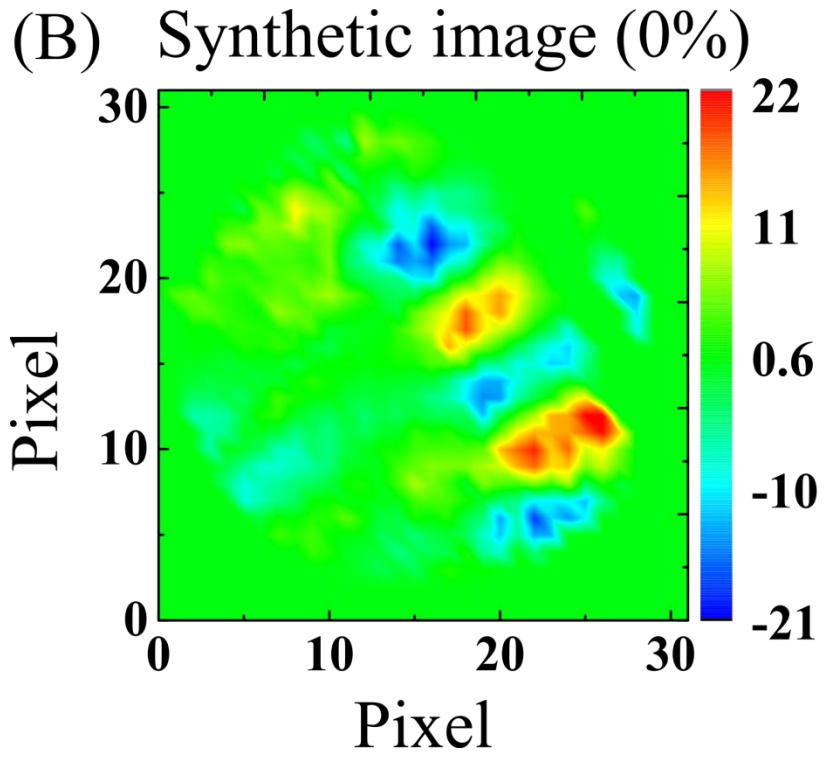

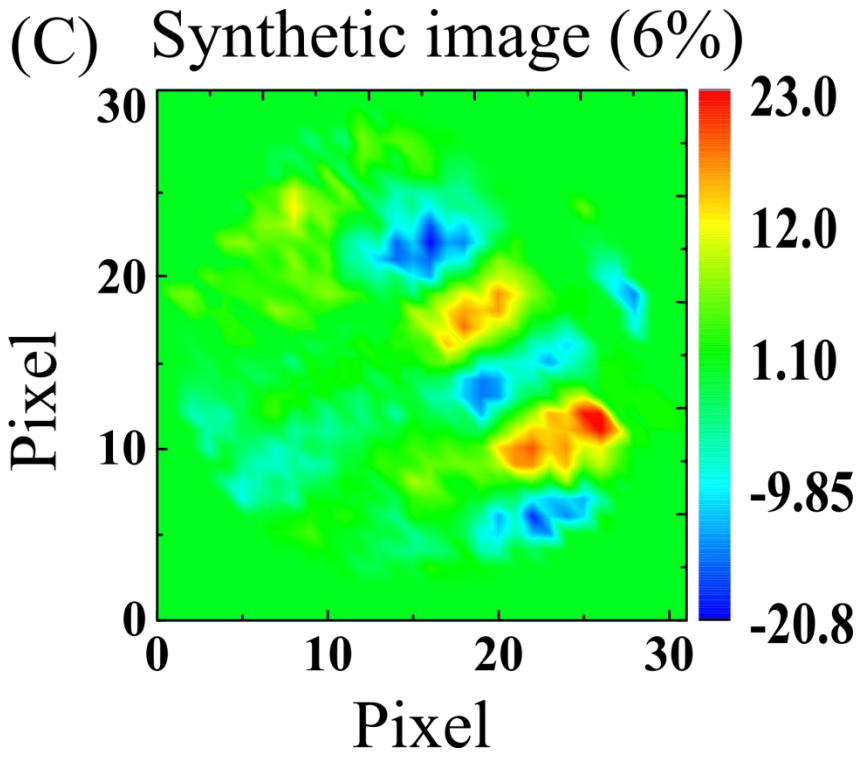

Reconstructed mode structure

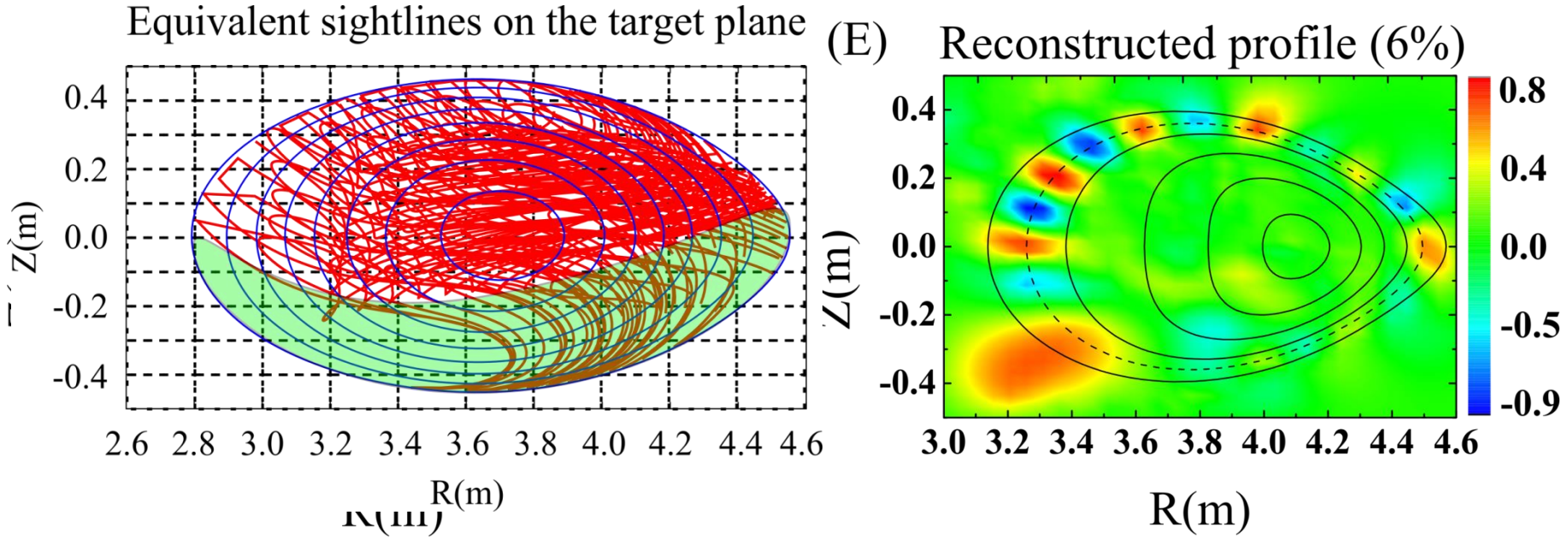

- Mode structure with high mode number can be reconstructed in LHD configuration.
- VUV imaging system can be a potential tool to reconstruct the 2D mode structure with high mode number for LHD plasma in future.

Tingfeng MING, et al, Plasma Fusion Res. 6, 2406120 (2011).

Outline

- Background and motivations
  - Merits of tangentially viewing imaging system
  - Tangentially viewing VUV imaging system in LHD
- Image reconstructions
  - Relation of line-integrated image and local emission profile
  - Construction of geometry matrix
    - One-dimensional array
    - Tangentially viewing imaging system
  - Synthetic image with a plausible emission profile
- CT reconstruction by numerical tests with LHD configuration
  - Iwama's type of P-T algorithm
  - Numerical test results
- Experimental results
  - Observation of the distorted emission profile caused by ELM event
- Summary

Emission profiles & line-integrated images

$$E(\rho,\theta) = exp\left[-\left(\frac{\rho-\rho_p}{w}\right)^2\right] cos(m\theta+\phi_0)$$

- Comparisons of synthetic images and experimental data are performed.
- ρ_p, w, m, ϕ_0 are scanned to search the plausible mode structure.

$$d^2 = \frac{1}{N}\sum_n (I_n - I_n^*)^2$$

is defined to clarify the similarity of the synthetic and experimental images.

Emission profile

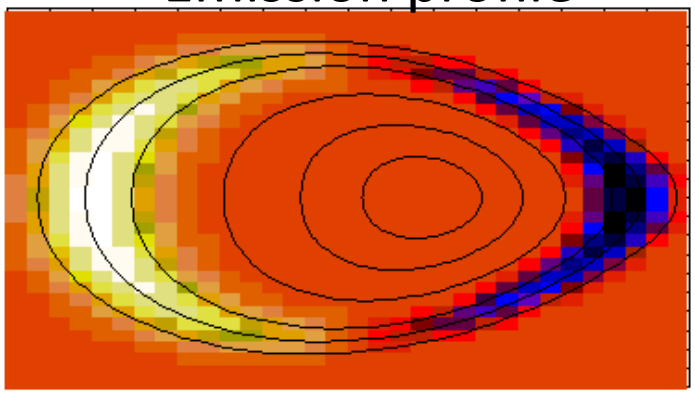

Experimental

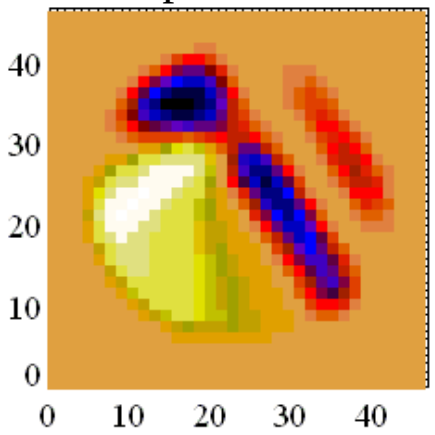

Synthetic

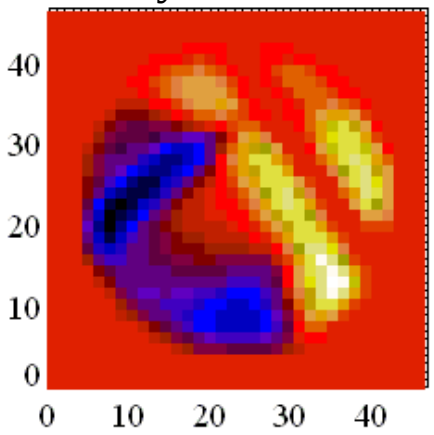

Relative errors

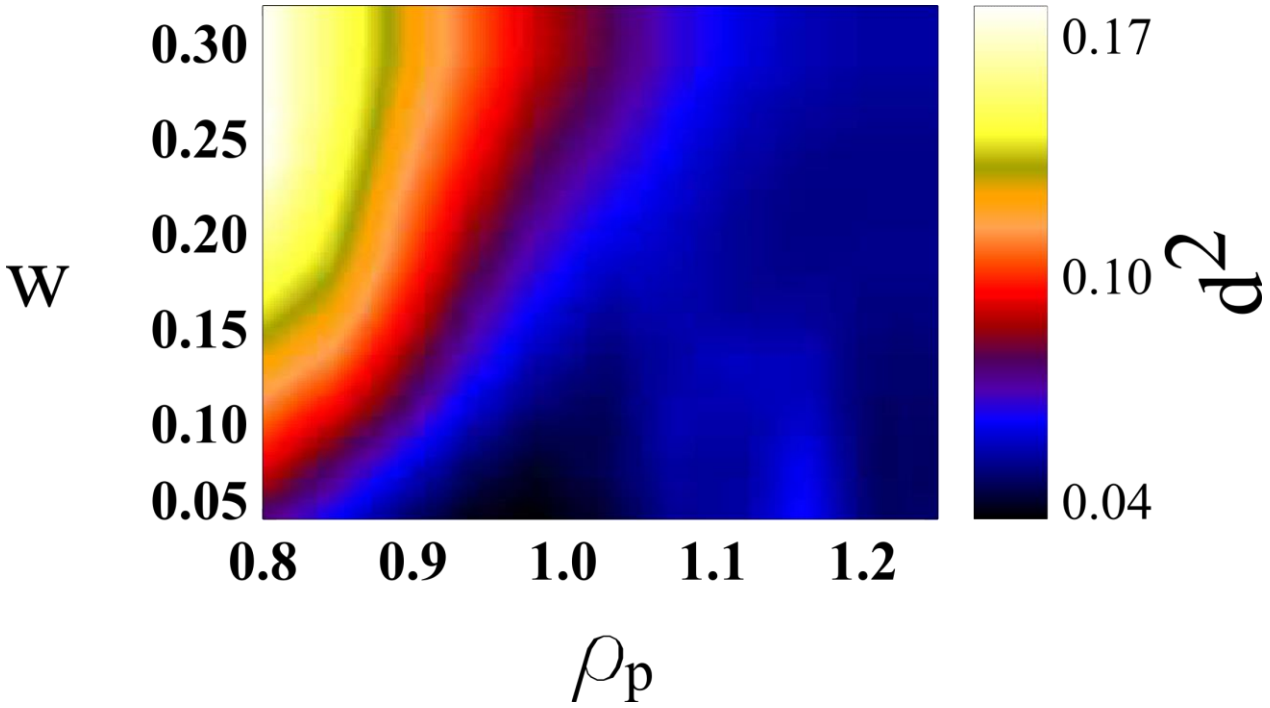

➢An optimized combination of w and ρ_p gives a minimum d^2 .

Plausible emission profiles estimated from experinemtal measured images

	U1	U2	U3	U4
	1.2r0.15wr	0.92r0.15wr	0.92r0.15wr	1.25r0.22wr
Experimental images	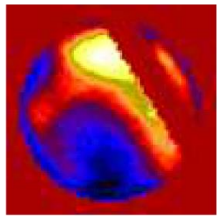	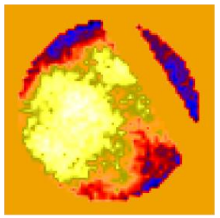	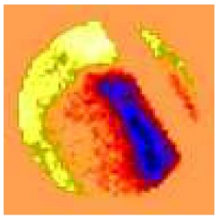	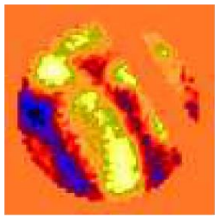
Synthetic images	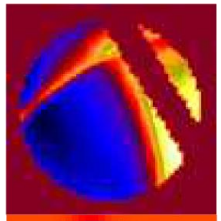			
Emission profiles	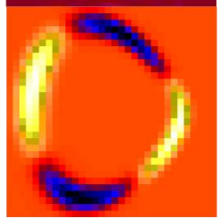	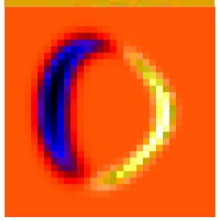	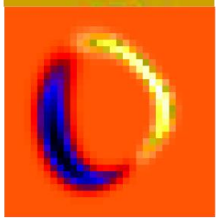	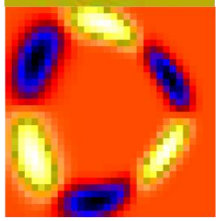
$d^2=$	0.05	0.07	0.03	0.08

Summary

- A new method based on the HINT2 equilibrium code is developed for constructing the geometry matrix for a tangentially viewing imaging system. It can be used with finite beta plasma.
- Numerical tests based on the Iwama's P-T algorithm show that mode structures with high mode number can be reconstructed even with a complex shape of LHD plasma. (*Tingfeng MING, et al, Plasma Fusion Res. 6, 2406120 (2011).*)
- Plausible emission profiles caused by ELM crash have been estimated by comparing sythetic images and experimental measurement.

Thank you for your attention!

Observation of the distorted mode structure

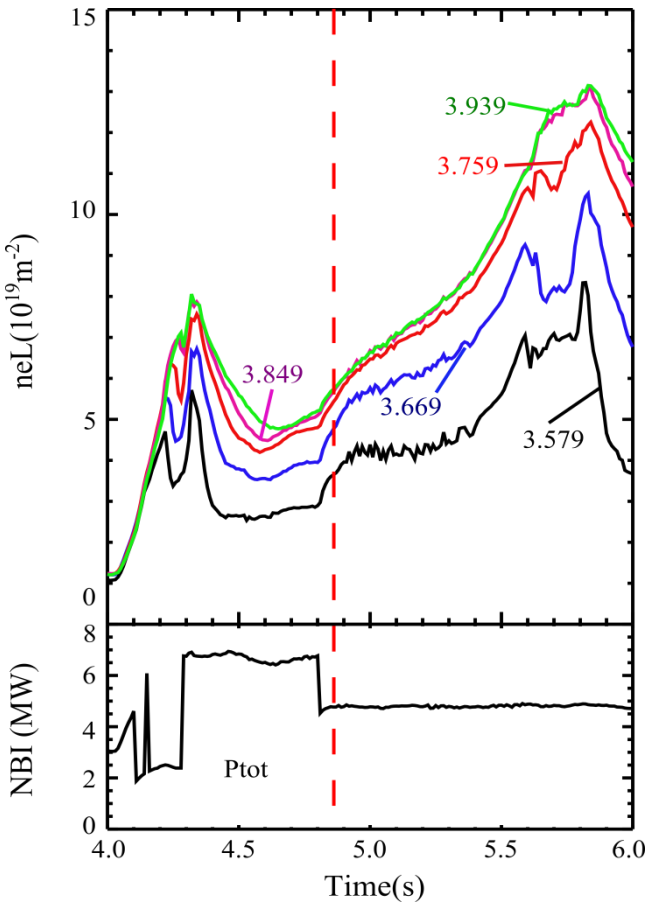

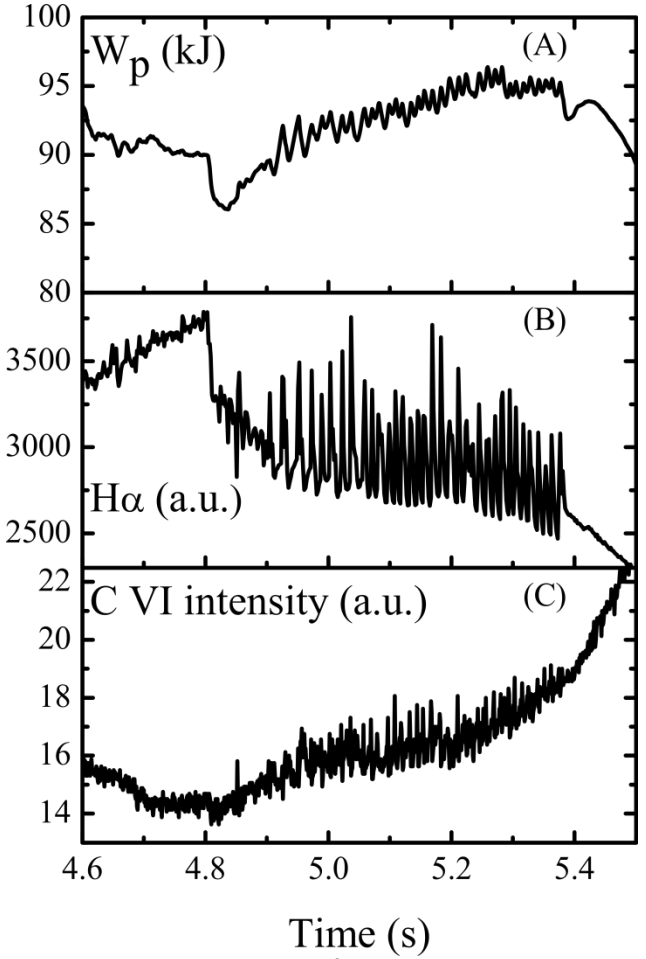

(Rax=3.95m, Bt=-1.0T,gamma=1.254)